CUKUROVA UNIVERSITY

INSTITUTE OF NATURAL AND APPLIED SCIENCES

MSc THESIS

ARTIFICIAL INTELLIGENCE UTILIZED BALLISTOCARDIOGRAPHY AND PHONOCARDIOGRAPHY BASED BLOOD CLOT DETECTION SYSTEM

NADIM ALDARVISH

Biomedical Engineering Department

September, 2024

CUKUROVA UNIVERSITY

INSTITUTE OF NATURAL AND APPLIED SCIENCES

MSc THESIS APPROVAL

ARTIFICIAL INTELLEGENCE UTILIZED BALLISTOCARDIOGRAPHY AND PHONOCARDIOGRAPHY BASED BLOOD CLOT DETECTION SYSTEM

NADIM ALDARVISH

Biomedical Engineering Department

This Master's Thesis was evaluated by the following Jury Members on 02/09/2024 and was approved by unanimity / ~~majority~~ of votes.

Jury : Prof. Dr. Mutlu AVCI (Advisor) ……

: Assoc. Prof. Dr. Zehan KESİLMİŞ ……

: Asst. Prof. Dr. Mustafa İSTANBULLU ……

This Thesis was written in the Department of Biomedical Engineering, Institute of Natural and Applied Sciences.

Thesis Number:

Prof. Dr. Sadık DİNÇER
Director
Institute of Natural and Applied Sciences

CONTENTS

CUKUROVA UNIVERSITY
INSTITUTE OF NATURAL AND APPLIED SCIENCES

MSc THESIS

ARTIFICIAL INTELLEGENCE UTILIZED BALLISTOCARDIOGRAPHY AND PHONOCARDIOGRAPHY BASED BLOOD CLOT DETECTION SYSTEM

NADIM ALDARVISH

Advisor: Prof. Dr. Mutlu AVCI

Department of Biomedical Engineering

ABSTRACT

Heart attacks and strokes are some of the leading causes of death in the world. Both of these diseases are usually the outcome of blocked arteries caused by blood clots.

The presented innovation is about using a set of sensors and a trained artificial neural network (ANN) to detect and locate the blood clots across the body. The mentioned sensors will be placed under the patient's bed, then ballistocardiography (BCG) signals will be measured and transferred to the phonocardiography (PCG) system, where they will be converted into sound signals. BCG and PCG graphics will be seen on the output display of the system; the obtained BCG and PCG signals will be fed into a trained artificial neural network, which will locate the locations of blood clots in the body's vessels.

Keywords: BCG, PCG, ANN, blood clots.

ÇUKUROVA ÜNİVERSİTESİ
FEN BİLİMLERİ ENSTİTÜSÜ

YÜKSEK LİSANS TEZİ

YAPAY ZEKA DESTEĞİ İLE BALLİSTOKARDİOGRAFİ VE FONOKARDİOGRAFİ SİNYALLERİNE DAYALI KAN'DA PIHTI TESPİT SİSTEMİ

NADIM ALDARVISH

Danışman: Prof. Dr. Mutlu AVCI

Biyomedikal Mühendisliği Anabilim Dalı

ÖZ

Kalp krizleri ve beyin inmeleri dünyanın en çok ölüme sebep olan hastalıklardır, genellikle her ikisi kan pıhtıları ile tıkanan damarların sonucudur.

Buluş, damarlardaki oluşan kan pıhtıların yerlerini tespit etmek amacıyla bir sensör matrisi ve eğitilen bir yapay sinir ağı (ANN) desteği ile ilgilidir. Buluşta, hastanın yatağının altına bir sensör matrisi yerleştirilecektir, ballistokardiyografi (BCG) sinyalleri ölçülüp fonokardiyografi (PCG) sistemine aktarılacak, PCG sistemine aktarılan sinyaller ses sinyallerine dönüştürülecektir.Sistemin çıkış ekranında hem BCG hem de PCG sinyallerin görünecektir, elde edilen BCG ve PCG sinyalleri eğitilen bir yapay sinir ağına aktarılıp vücut damarlarındaki kan pıhtıların yerleri tespit edilecektir.

Anahtar Kelimeler: BCG, PCG, ANN, kan pıhtıları.

ACKNOWLEDGEMENTS

I would like to thank my supervisor, Prof. Dr. Mutlu AVCI, for his patience and faith in me. His guidance and advice made this work possible. My gratitude also goes to our department's academic members for all their insight and support. I would also like to thank Çukurova University for providing all the facilities and a healthy environment.

Finally, I would like to thank my family, friends, and everyone who believed in my capabilities and abilities.

LIST OF TABLES

LIST OF FIGURES

SYMBOLS AND ABBREVIATIONS

BCG : Ballistocardiogram / Ballistocardiography
PCG : Phonocardiogram
ANN : Artificial Neural Network
AI : Artificial Intelligence
MMOCT : Magnetomotive Optical Coherence Tomography
PAFC : Photoacoustic Flow Cytometry
CBCs : Circulation Blood Clots
ECMO : Extracorporeal Membrane Oxygenator
MES : Microembolic Signals
RBCs : Red Blood Clots
NIR-II : Second Near-Infrared
2D CNN : Two-Dimension Convolutional Neural Network
LRR : Light Reflection Rheography
DVT : Deep Vein Thromboses
ECG : Electrocardiogram / Electrocardiography
CCNN : Cascaded Convolutional Neural Network
ReLu : Rectified Linear Units
CNN : Convolutional Neural Network
CAD : Computer Aided Diagnosis
CAD : Coronary Artery Disease
RBM : Restricted Boltzman Machine
DBN : Deep Believe Networks
ABP : Arterial Blood Pressure
EMG : Electromyogram / Electromyography
AR : Autoregressive
TI : Thoracic Impedance
OHCA : Out-Of-Hospital Cardiac Arrest
PR : Pulse-Generating Rhythm
PEA : Pulseless Electrical Activity
SVM : Support Vector Machine
TC : Total Cholesterol
BIA : Bioelectrical Impedance Analysis

BMI : Body Mass Index

MI : Myocardial Infraction

VHD : Valvular Heart Diseases

AS : Aortic Stenosis

MS : Mitral Stenosis

MR : Mitral Regurgitation

MVP : Mitral Valve Prolapse

MODWT : Maximal Overlap Discrete Wavelet Transform

RNN : Recurrent Neural Network

BiLSTM : Bi-Directional Long Short-Term Memory

HSAD : Heart Sound Activity Detection

SCG : Seismocardiogram / Seismocardiography

PSG : Polysomnography

HPT : Hypertension

BP : Blood Pressure

CWT : Continuous Wavelet Transform

HC : Healthy Controls

CV : Cross Validation

CMRR : Common Mode Rejection Ratio

IC : Integrated Circuit

PWM : Pulse-Width Modulation

INA : Instrumentational Amplifier

PA : Power Amplifier

HPF : Hight Pass Filter

LPF : Low Pass Filter

BPF : Band Pass Filter

NI : Non-Inverting

OP : Operational

Amp : Amplifier

MLP : Multilayer Perceptron

CSV : Comma-separated values

RAF : Raw Fujifilm

HRV : Heart Rate Variety

1. INTRODUCTION

A blood clot is the outcome of blood coagulation in hemostasis. It is a defensive mechanism for injuries intended to stop and prevent further bleeding but can be harmful if it is formed inside the blood vessels, which might lead to many complex issues later.

There are two types of blood clots: microclots and mural thrombi. Microclots are formed in the smallest blood vessels, the capillaries; they can obstruct the blood flow in those capillaries, which can lead to many problems, such as affecting the alveoli in the lungs and reducing the oxygen supply of the body tissues. Mural thrombi are blood clots that adhere to the wall of large blood vessels; they are most commonly found in the aorta. They can obstruct blood flow but usually do not block it entirely; mural thrombi are usually found in damaged vessels; they can be separated from the chamber of the heart or from the walls of blood vessels and get carried with the blood flow through arteries and block blood vessels. If a blood clot dislodges and starts to flow, it is considered an embolus; if an embolus becomes trapped within a blood vessel, it will cut off the blood supply and might lead to many fatal complications and even death.

While the BCG is a technique used to detect the vibrations resulting from the contracting and stretching of the blood vessels each time blood flows with every heartbeat, PCG is a technique used to capture and record heart and blood flow sounds. In this study, an artificial intelligence utilized BCG and PCG-based measurement system is proposed to detect and locate blood clots during the sleep phase. A set of sensors will be placed under the patient's bed. During the sleeping phase, those sensors will be measuring and recording BCG signals across the body; the recorded BCG signals will be later fed to the PCG system, which will convert those signals into sound signals. As a result, multiple graphics will be obtained from the BCG and PCG signals. An Artificial neural network (ANN) will be trained with the BCG and PCG signals. If there is a moving blood clot in the blood, it will disrupt the BCG and PCG signals in the nearest measurement point, and the ANN will be able to detect and locate the blood clots.

The difference between this study and the previous studies is not just by using a non-invasive no skin contact technique but by performing the technique during night sleep which will make it possible to collect much more data and make it monitorable and controlled by AI. The study and the experiments were done in a laboratory environment. This method is not in the literature. Integrating this system into beds in both hospitals and houses and using it in daily life will make the detection of blood clots much easier and more efficient.

2. PRELIMINARY WORK

Many studies and research have been done on this topic. A new biosensor was invented for blood clotting biomarker detection. The new biosensor can detect the blood clotting factor IX protein, which means it can detect blood clots in the early stages. (Krishnan et al., 2022)

Magnetomotive optical coherence tomography (MMOCT) and labeled platelets were used to detect blood clots and measure their elasticity. The used platelets were rehydrated, lyophilized, and loaded with super-magnetic iron oxides that adhere to sites of vascular endothelial damage. After that, the MMOCT was used to locate the blood clots by locating the functional platelets. (Oldenburg et al., 2011)

Fourier transform mechanical spectroscopy was used to detect incipient blood clots in samples of human blood. (Evans et al., 2008)

Phantoms and chemical activations of clotting were employed in rabbits and rats. These procedures were described as microsurgical. The mentioned procedures were applied in different ways, such as inserting a catheter or a needle to inject an artificial clot, which would be the equivalent model to a real stroke. An in vivo photoacoustic flow cytometry (PAFC) was demonstrated as a detection method of circulated blood clots (CBCs) by using focused ultrasound transducers. (Juratli et al., 2018)

Blood clot detection was also achieved by using magnetic particle spectroscopy (MSB) via specific binding of aptamer functionalized magnetic nanoparticles with the blood clot. Those nanoparticles have different bounding states with different relaxation times. The produced harmonics by those nanoparticles are used to measure the rotation freedom and, therefore, the bound state of the nanoparticles, and by doing so, when those particles bound to thrombin in the blood clot, it will produce different harmonics with different relation times that will be detected by the MSB. (Khurshid et al., 2017)

A different type of imaging system was used to detect blood clots in the brain. The system basically consists of a microwave head antenna that sends electromagnetic waves to the head. The head itself was divided into four equal sections, whereas the microwave antenna was placed at different positions in front of each one of those four sections. The reflected signals from the head are accumulated and processed, which will be helpful later to reconstruct an image of each one of the four sections of the head. At the end, four different images from four different sections of the head will be obtained, and the four images will be compared based on the intensity of the reflected waves. Any difference in the intensities will be alarming to the clinicians. Higher intensities of the reflected waves will be helpful enough to detect any potential blood clots. (Parveen and Wahid, 2022)

In extracorporeal membrane oxygenators (ECMO) system, bedside sound measurements and additional laboratory experiments were used to show that it is possible to detect blood clots or fragments of clots by analysing the strength of infrasound modes of the spectrum near the inlet and

outlet of the centrifugal pump in the ECMO system, a laboratory setup provided insight of the flow in and out the pump, confirming that in the presence of particles a low amplitude low-frequency signal is strongly amplified which indicates the identification of a clot. (Fuchs et al., 2016)

As many diseases are associated with heat, infrared thermal imaging was used as a pre-screening test in the diagnosis of deep vein thrombosis with developed computer-aided software. Therefore, patients can be treated quickly and correctly because the time lost is minimized and unnecessary treatments are avoided. (Kacmaz et al., 2017)

Transcranial Doppler techniques are unique when it comes to the detection of microembolic signals (MES) in cerebral circulation. Presence and amount of MES can identify a high-risk status in the setting of potential arterial or cardiac sources of cerebral embolism. (Topcuoglu and Arsava, 2012)

A system consisting of a pressure transducer, microprocessor, analytical line, aspiration line, and a valve was made to detect blood clots. The pressure transducer is connected to the aspiration line to provide output voltage corresponding to the vacuum level during the aspiration process. The microprocessor measures the vacuum reading for each aspiration cycle for each test sample and a pressure value is determined for a cycle without any clotting to be used as a reference value. A valve is provided across the analytical line and the aspiration line to allow or prevent communication between the mentioned lines. The communication between the two lines permits the transfer of a test sample from the aspiration line to the analytical line if the test sample is considered acceptable for sample analysis. If there was a difference in pressure between the test sample and the reference value, then the sample will be transferred to the analytical line. (Gherson et al., 2000)

A photoacoustic technique was used to recognize the aggregated red blood clots (RBCs) from the non-aggregated RBCs. By using a pulsed laser to obtain the power of photoacoustic signals, it can also estimate the viscosity of blood before and after the process and show the shape, size, and number of RBC clusters. (Hameed et al., 2022)

A polymer nanoplatform that integrates long-wavelength second near-infrared (NIR-II) photoacoustic imaging-based was developed to detect thrombosis. The mentioned nano platform was formulated by designing and synthesizing a semiconducting homopolymer with strong absorption in the NIR-II region and molecular motion that boosts photothermal conversion and photoacoustic signal; then the homopolymer gets doped with a thermosensitive nitric oxide donor. As for thrombus targeting, a fibrin-specific ligand was functionalized. With a strong NIR-II light, bright photoacoustic signal, and active thrombus accumulation, it was noticed that the NIR-II nanoprobes were able to detect thrombi successfully, and it was also noticed that the nano platform has a rapid and efficient blood clot removal ability in both carotid thrombosis models and low extremity arterial thrombosis models. (Song et al., 2023)

A neural network model was used to determine the disease based on the patient's symptom inputs. The test was done with the help of the MATLAB `nftool` with a high accuracy. The

mentioned system would take blood clot symptoms as user input and provide the type of blood clot disease they are suffering from so that the patient can go to the hospital for further diagnosis. (Sanders and Reddy, 2007)

A two-dimension convolutional neural network (2D CNN) to evaluate the qualities of light reflection rheography (LRR) signals and classify the positive or negative deep vein thromboses (DVT) from the LRR signal with high reliability, which will make the daily monitoring of the DVT in the lower limbs possible. (Liu et al., 2021)

An examination system was developed to be used at non-medical places to detect the DVT of lower limbs with light reflection rheography (LRR); the system basically consists of a wearable device and a mobile application; it controls the sensors wirelessly and displays and stores the LRR signals on the APP. A cuff was used to apply pressure on the veins of the lower limbs by 100 mmHg and 150 mmHg to stimulate the slight and serious DVT scenarios. The experimental results show that the proposed examination system may be practical for screening DVT in a homecare environment. (Liu et al., 2022)

A convolutional neural network was presented to encode a single QRS complex with the addition of entropy-based features. The obtained data from the PTB-XL database, which includes raw ECG signals, entropy-based features computed from raw ECG signals, extracted QRD samples, and entropy-based features computed from extended QRS complexes, was used to determine the combination of signal information in order to classify ECG signals. (Śmigiel et al., 2021)

A cascaded convolutional neural network (CCNN) and expert features were used to classify a 12-lead ECG arrhythmia. A one-dimensional (1-D) CNN is designed to extract features from each single-lead signal; then, features are cascaded as input to two-dimensional (2-D) densely connected ResNet blocks to classify the arrhythmia; later on, features based on expert knowledge are extracted, and a random forest is applied to get a classification probability. In the end, a stacking technique is used to combine results from both CCNN and expert features as the final classification result. (Yang et al., 2021)

Since arrhythmia has different levels of danger and threat, it can be divided into different categories. A novel deep learning method was suggested to arrange the different types of arrhythmias; the suggested method works in regard to the deep residual network (ResNet). The structure of this algorithm is divided into four residual blocks, each one of them consisting of convolutional layers, rectified linear units (ReLu) layers, batch normalization (BP), and a shortcut connection structure. A 2-lead ECG was combined with the mentioned method to recognize the different types of heartbeats. The results were satisfying, and the suggested method showed promise in the classification field. (Li et al., 2020)

A convolutional neural network (CNN) method with many layers was utilized to detect different types of heartbeats extracted directly from the ECG signals. The suggested method uses 9 layers of CNN, and the raw ECG signals were derived from a public database. The environment of

the experiment was a noisy environment with multiple sets of data. The imported data of ECG signals were passed through a filtering system to get rid of the high-frequency noise. The algorithm was trained with the ECG data sets. The suggested method achieved good results regarding the classification of the different types of heartbeats. (Acharya, Oh, et al., 2017)

Two segments of the ECG signals were used to automatically classify the ventricular arrhythmias into two different categories regarding whether or not a shock should be used. A convolutional neural network (CNN) with multiple layers was used to process the obtained segments of the ECG signals. The suggested system achieved high results in accuracy, sensitivity, and specificity, which shows that it can immediately detect life-threatening arrhythmia. (Acharya et al., 2018)

ECG signals were evaluated and made sure to be accurate and objective by using a computer-aided diagnosis (CAD). A new technique suggested that the different segments of the ECG signals can be detected automatically by a convolutional neural network (CNN). There are twelve layers that construct the algorithm; eleven of them are deep convolutional layers, and the last layer is the output layer. The normal, atrial flutter, ventricular fibrillation, and atrial fibrillation ECG classes were represented in those layers. For a two-second duration and a five-second duration, the ECG signals were tested, and no QRS complexes were detected in those tests. The suggested technique shows promise in helping clinicians and assisting them when it comes to the confirmation of the diagnosis they make. (Acharya, Fujita, Lih, Hagiwara, et al., 2017) In another study convolutional neural network structure was also used to detect coronary artery disease (CAD) using ECG segments with various durations. Eleven layers construct together the structure of the suggested method; those layers can be classified as convolutional layers, connection layers, and pooling layers. The algorithm uses a duration of two seconds in one test and a duration of five seconds in another test for the diagnosis of CAD with the use of different segments of the ECG signals. In a similar conclusion to the previous study, the convolutional neural network was found helpful to clinicians in detecting CA. (Acharya, Fujita, Lih, Adam, et al., 2017)

A deep learning methodology-based novelty was presented to classify ECG signals. The type of measured ECG signals were single-lead measurements. To classify those signals, both the deep belief network (DBN) and the restricted Boltzmann machine (RBM) were applied. The MIT-BIH database was the source of the ECG signals. The combinational use of RBM and DBN with a sampling rate that is considered as low as 114 Hz shows that it is possible to recognize different beats of the heart, such as ventricular ectopic beats and super ventricular ectopic beats. The combination of those methods provided the needed power for the classification process. As mentioned before, this technique uses a low sampling rate and simple features, which is a big advantage. As this technique shows promising results, it can also be used in other fields, such as arterial blood pressure (ABP), heart rate variability (HRV), and nerve conduction (EMG). (Mary et al., 2018)

Electromyography (EMG) is a complex signal consisting of multiple sub-signals; each one of those sub-signals is generated from a different group of muscles, and in the same way, each of these sub-signals supports a unique motion related to the arm and the fingers. To classify those signals, an artificial intelligence-based classifier method with other parameters was utilized to recognize the different types of those sub-signals. Many of the EMG signal features were extracted from multiple segments. For each one of those features, a reference value was declared; later on, the distance between the measured value and the reference value would be calculated. This method depends on the accumulation of evidence, and to achieve that, a fuzzy mapping function was used. (Park and Lee, 1998)

Both thoracic impedance (TI) and electrocardiogram (ECG) were used in an attempt to detect different types of pulse signals. A high number of ECG and TI segments were derived from a database of out-of-hospital cardiac arrest (OHCA) patients. Almost two-thirds of the data were assigned to pulse-generating rhythm (PR), whereas the last third was assigned to pulseless electrical activity (PEA) by a number of professionals. While the TI segments were extracted by an adaptive filter, the ECG segments were extracted and denoised by applying a wavelet function. The PR data would imply that there is a pulse, whereas the PEA data would imply that there isn't any pulse. The PR and the PEA extracted features were fed into a support vector machine (SVM) classifier to get the final results. The process was repeated many times to get the best results and the highest performance. In the end, this method was able to classify the pulse signals with a high accuracy, sensitivity, and specificity, which makes it a reliable method that can be used by clinicians in the future. (Alonso et al., 2020)

A new non-invasive technique was suggested to estimate the amount of total cholesterol (TC) levels in the blood. The technique is based on bioimpedance measurement and artificial neural network (ANN). A bioelectrical impedance analysis (BIA) was done to provide the input parameters that will be used by the ANN. The BIA analysis was done non-invasively. A number of volunteers participated in the study. More than %73 of the obtained data was used to train the ANN, whereas the rest of the data was used for the actual test. Six different parameters were extracted from the BIA and those parameters were used to detect TC levels in blood. Multiple ANN techniques were applied to test the TC levels; later on the obtained results from those techniques were compared together to get the most accurate value, (Mohktar et al., 2013)

A novel method suggested that electrocardiogram (ECG) segments can be used as parameters to assign the myocardial infraction (MI) automatically. Two main signals were used in this study: the normal ECG signals and the problematic MI signals. The obtained signals were in both noisy and denoised forms. In this method, there was no need for any feature extraction. The results were satisfying and enough to give the professionals good support with the diagnosis they do on a daily basis. (Acharya, Fujita, Oh, et al., 2017)

Phonocardiogram (PCG) signals were used to detect valvular heart diseases (VHD) based on deep learning techniques. Different types of heart sounds, including normal sounds and abnormal sounds, are related to different kinds of diseases. The collected heart sounds were derived from an open-source database. Different types of processes, from filtering and smoothing up to normalization, were done to the collected sound signals. Both convolutional neural network (CNN) and recurrent neural network (RNN) were used together as a one artificial neural network structure to simplify what was found in the literature. This method could be a potential milestone towards the use of ANN methods to detect and classify the different types of VHD and help clinicians in diagnosing the different types of cardiac diseases. (Alkhodari and Fraiwan, 2021)

Unlike other heart sound analysis and diagnosis methods, which use parameters measured from the PCG signal such as amplitude, frequency, period, the shape of the signal, and the different types of signals. This method uses different systems such as filtering, computing, boundary assignment, and a modified location of the boundary. The kind of classification that this method provides basically classifies the signals into a clean and noisy signal and also into safe, regular, and abnormal dangerous PCG signals. This method succeeded in achieving its goals by being able to determine the different acoustic effects without the need to use any complex techniques but rather by being very direct and powerful. (Varghees and K I, 2014)

While the ECG provides details about the electricity of the heart, it can only predict abnormalities related to the heart rhythm, and measuring the ECG signal can be difficult when it comes to infants. While the ECG signal can be totally fine and show no problems with the electricity of the heart, problems, and diseases related to blood and blood vessels can cause serious or even fatal damage. The PCG can detect and analyse heart sounds. Heart sounds can give a good idea about the cardiac cycle, so whenever there is an abnormality with the heart, one of the heart sound signals gets distorted, or the abnormality itself can be shown as a new signal, which can be referred to as a murmur. In this study, PCG signals were measured and fed into a classification system to separate the normal heart sounds from the abnormal heart sounds. This method is very direct, simple, and easy to implement. (Singh and Cheema, 2013)

A non-invasive system was presented to detect and process PCG and ECG waveforms. The system consists of an electronic acoustic stethoscope and a server computer. While the heart sounds are measured by using an acoustic transducer of a chest piece and then sent to an earpiece of the stethoscope, the electrical signals of the patient's heart are measured by using at least four electrodes of the chest piece; the obtained PCG and ECG signals are then transmitted to a server computer by a wireless communication device to be processed for additional information. (Chen and Yang, 2018)

The advancement in technologies made it possible to measure the Ballistocardiogram (BCG) and the Seismocardiogram (SCG) in different places outside of the clinical environment. The different mechanisms, methods, and engineering structures have made many upgrades related to noise reduction, better feature selection, and forming signals. Due to the mentioned achievements, a

new medical reality was shaped where scientific studies can take place and give more promising results than ever. When the heart beats, blood passes to the different types of tissues and organs of the body through the different types of vessels, and that creates vibrations across the body. Those vibrations are the result of the micromovements that happen in every part of the body. In reaction to those micromovements to keep the whole system in balance, recoil forces are produced. The Ballistocardiogram (BCG) is the measurement and recording of those recoil forces. There are different types of methods to measure the BCG and there are also different types of sensors that can be used to detect the BCG vibrations. There are also different axes where the BCG signals can be measured. Measuring the BCG signals from different places of the body would produce different BCG signals that are slightly different from each other, but they all consist of the same structure and the same segments. The type of sensor that would be used, the method that would be applied, and the axes of the measurement should all be chosen based on the goal of the study. Compared to other signals, the BCG signal has more advantages, such as taking measurements during sleep phases, and it is also contactless and non-invasive, which will automatically get rid of the artifact noises. BCG signals can be monitored, and they can provide a lot of help to clinicians due to the information they carry. Just like the BCG can be measured in hospitals and clinics, the BCG signals can also be measured in a home environment. (Inan et al., 2014)

A new device was presented to measure the BCG at the head behind the ear; the mentioned device looks similar to hearing aid devices. The BCG device has a wireless module, a three-axis mems accelerometer, and an analog signal processing block. It measures the BCG signals and transmits them to a PC where the transmitted signals get processed and recorded for further analysis. It should be noted that the measured BCG signal from the head is not quite the same as the traditional signal, but they both have a lot of similarities, and they share the same structure, such as the J waves. J wave numbers are directly related to the frequency of the heartbeats; the more heartbeats, the more J waves are produced. It is also possible to synchronize both the BCG and ECG signals and study the RJ interval. The RJ interval provides a lot of useful information about the cardiac cycle. The advantages of this device are mostly that the device is portable, wireless, real-time measurement support, and is friendly user. (He et al., 2012)

Both the Ballistocardiogram (BCG) and Seismocardiogram (SCG) have been studied for a fair amount of time; during that time, it was clear that those signals carry a lot of beneficial information about the cardiovascular system and the cardiac cycle. At the same time, it was noticed that those same signals can be affected by many factors, such as respiration. To get rid of the respiration effect, digital filters and other structures were developed and applied. The aim of this study is to shed light on the interaction between the cardiovascular system and the respiratory system based on the BCG and SCG signals. Different sensors and transducers were used in those experiments to get the best results. The respiratory signal was extracted to study sleep disorders. As mentioned before, the BCG and the SCG signals can be affected by many factors, and whatever

method is used, it's not possible to remove all the artifacts, but instead, it can be reduced. With the help of artificial intelligence, it is even more possible to get cleaner signals, which will impact the diagnosis made. The results of this study were promising and implied that both the BCG and the SCG signals can replace the old standards and provide better diagnosis, not to mention other advantages related to time and cost. (Balali et al., 2022)

Hypertension (HPT) is widely common among people, and it is considered a risk factor for many serious diseases; that is why controlling HPT is one of the challenges that humanity faces. HPT has many alarming symptoms, such as severe headaches, chest pain, vomiting, dizziness, and many others. There were some achievements regarding blood pressure (BP) measuring and using medicines that help with HPT. However, HPT is still a serious concern in the public eye. It is known that untreated HPT can lead to many fatal situations and complications, such as heart attack, stroke, heart failure, and many other cardiovascular diseases. Despite the seriousness of HPT, it doesn't show any strong symptoms in the early stages, and its early symptoms can be labeled as normal, non-dangerous signs that would be gone with time and rest; that is why it is difficult to detect HPT in the early stages. In this study, Ballistocardiogram (BCG) signals were used to detect HPT. Artificial intelligence was utilized to make it even easier. The BCG signals get processed, and after that, a continuous wavelet transform (CWT) would be used to convert the BCG signals into scalogram images. A 2-D convolutional neural network (2-D CNN) model was used to process the results of the CWT. The CNN was trained to classify the BCG signals into two main categories. The first category is the healthy category of patients who don't suffer from HPT whereas the second category is the category of the patients who suffer from HPT. This method achieved good results regarding accuracy. (Rajput et al., 2021)

3. MATERIAL AND METHOD

3.1. Materials

3.1.1. Piezoelectric Transducer

The piezoelectric effect is known as the ability of certain materials to generate electricity when they are exposed to mechanical stress. A transducer is a device that converts one form of energy to another form of energy. The piezo word is a Greek word which means squeeze, the piezoelectricity is the electricity that results from an applied pressure. The piezoelectric transducer is a transducer that uses the piezoelectric effect as a working principle. The piezoelectric transducer consists of a solid crystal and two metal plates; the solid crystal takes place between the metal plates, and the crystal holds static electric charges within itself; when pressure or mechanical stress is applied to the transducer, the solid crystal releases the static electrical charges as a voltage. While the plate with the bigger diameter represents the negative terminal of the transducer, the smaller plate represents the positive terminal. There are many types of piezoelectric transducers with different diameters, characteristics, and shapes. They can also be made of different materials. The piezoelectric sensor used in this study is very thin and made of ceramic with a diameter of 25 mm; a resistor was added in parallel with the piezoelectric transducer to stabilize the output voltage of the transducer, the piezoelectric transducer with the parallel resistor constitutes the input of the first stage of the proposed system. A shielded cable was soldered to the piezoelectric transducer; shielded cable is known for its ability to serve as electromagnetic compatibility protection, it prevents the internal signals from interfering with other components, and in the same way, it also prevents the external signals from interfering with the internal signals. Figure 3.1. shows the equivalent circuit of the piezoelectric transducer.

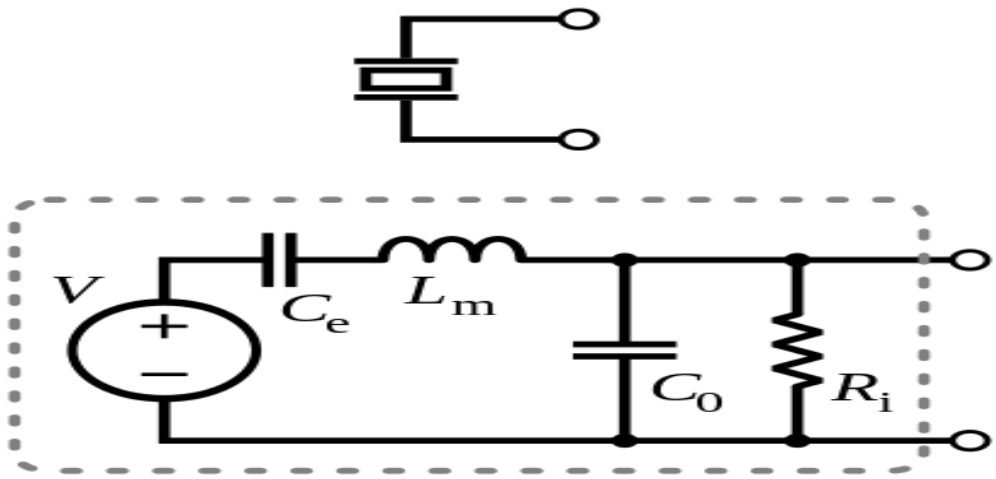

Figure 3.1. The equivalent circuit of the piezoelectric transducer.
Omegatron. 2007 (https://creativecommons.org/licenses/by-sa/3.0/)

3.1.2. The Instrumentational Amplifier Ina125

The instrumentational amplifier is a type of differential amplifier that can take two different inputs and reject any common signal among the inputs. This kind of amplifier consists of two stages input stage and the output stage; the input stage consists of two buffers that will get rid of the need for impedance compatibility as well as provide protection for the other stages of the circuit; the output stage consists of a differential amplifier. Since the instrumentational amplifier provides high input impedance, high common mode rejection ratio (CMRR), and high gain, it's suitable for medical applications. The instrumentational amplifier ina125 is a low-power, high-accuracy instrumentational amplifier with a precision voltage reference. As shown in Figure 3.2. The ina125 has its own gain formula whereas G = (4 + 60k/Rg), so basically, the gain of this instrumentational amplifier depends on the value of the resistor Rg. The output voltage Vo is calculated by calculating the difference between the input signals and then multiplying the result with the gain G. The ina125 integrated circuit (IC) shows better characteristics and properties compared to other instrumentational amplifier ICs. In the proposed system, the ina125 takes in the output signal of the piezoelectric transducer after it passes through the first buffer in the circuit. The other input of the instrumentational amplifier is connected to the ground, as we only have one input signal.

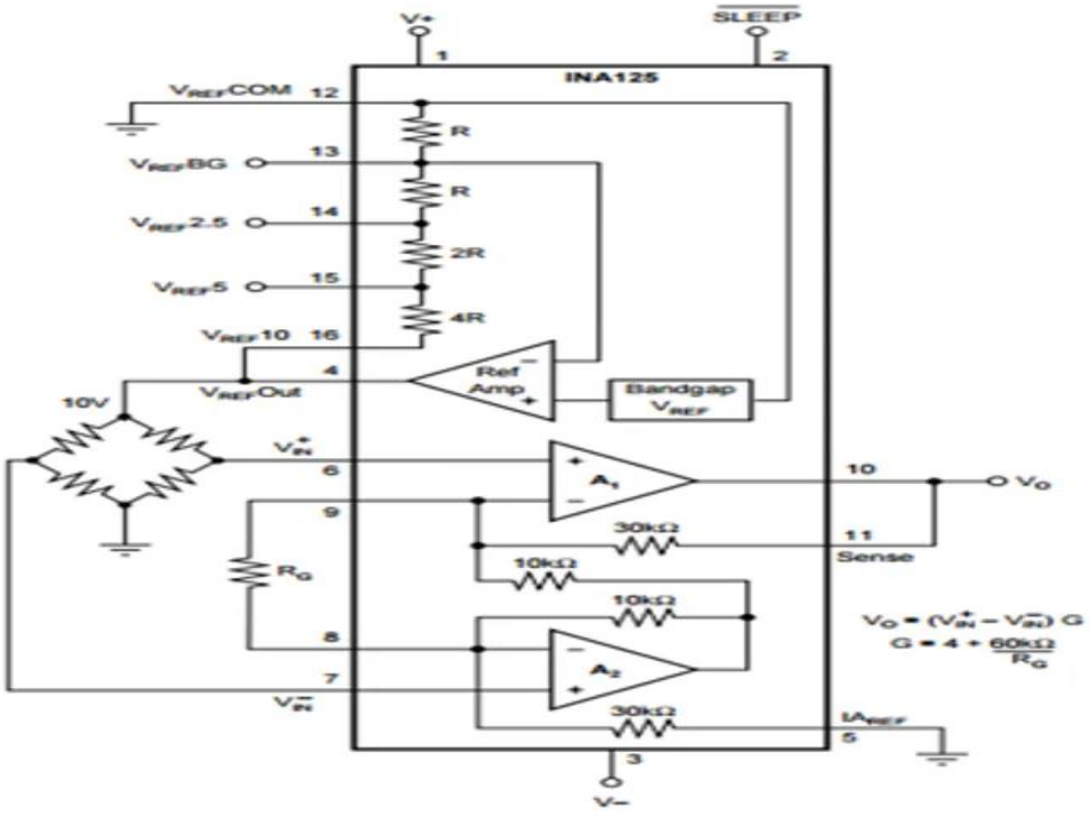

Figure 3.2. instrumentational amplifier ina125 IC structure.

3.1.3. Peristaltic Pump

A peristaltic pump is a mechanical pump that provides pressure by applying a constriction on a tube or hose; it is used to transfer different types of fluids from one place to another. As shown in Figure 3.3. The peristaltic pump consists of a pump casing, rollers or shoes, and a hose or tube. The fluid goes into the suction side, which is one of the tubes or hoses. The rollers inside the peristaltic pump apply a compress on the tube or hose while rotating, which will create a vacuum inside the tube or hose, which draws the fluid; at the end, the fluid goes out of the pump from the discharge side. Only the inner side of the tube or hose touches the fluid.

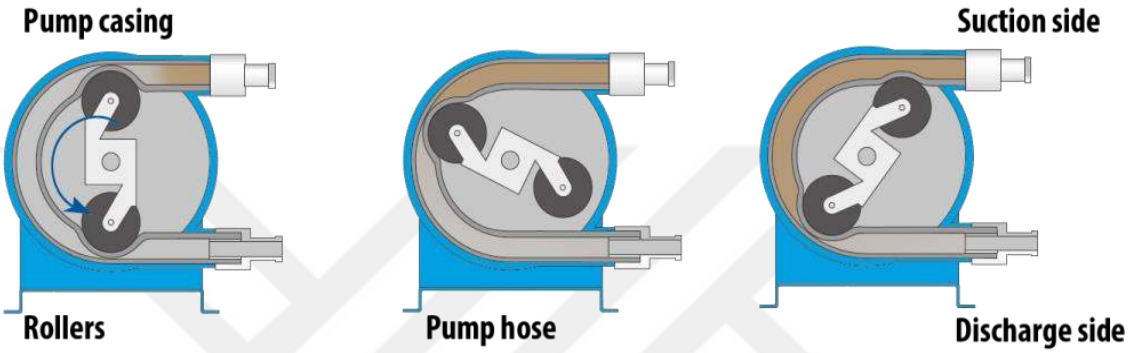

Figure 3.3. The working principle of the peristaltic pump.
https://www.tapflopumps.co.uk/blog/peristaltic-pump-guide/

The peristaltic pump needs electrical power to work; a motor driver is assembled to the pump for better control, and the speed of the pump is related to the PWM signal given to the motor driver. As shown in Figure 3.4, the motor driver circuit has multiple pins for control. Pins 1, 2, and 3 are digital pins, whereas 4 and 5 are analog pins. The analog pins can be used interchangeably, and with that, the suction side and the discharge side of the peristaltic pump would change places.

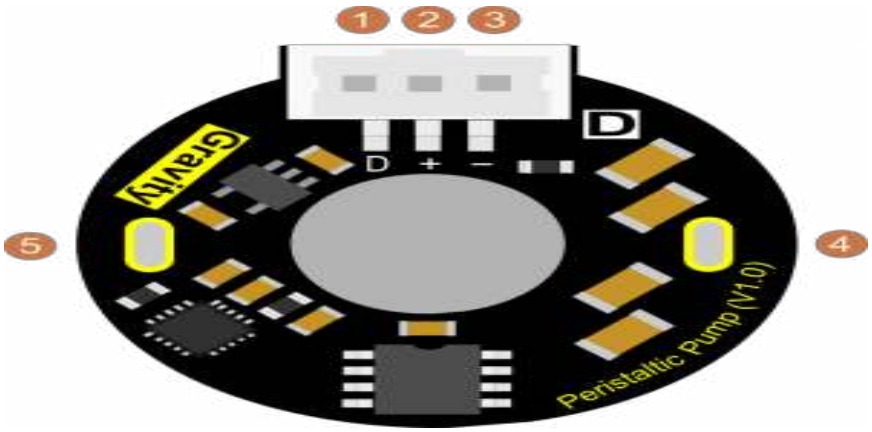

Figure 3. 4. The motor driver circuit pins.

The peristaltic pump used in this system is the DFR0532; as it was mentioned in the previous section, the peristaltic pump is a digital pump with a motor driver. The input voltage for the motor

driver is 5V-6V, the maximum operating continuous current is 1.8A, the quiescent current is 1mA, the flow rate of the fluid through the pump is 85ml/min, the rated power of the DFR0523 is 5W, as shown in figure 3.5. The peristaltic pump set consists of the actual pump, digital connectors, and a tube or hose made of the material BPT with an inner diameter of 3mm and an outer diameter of 5mm.

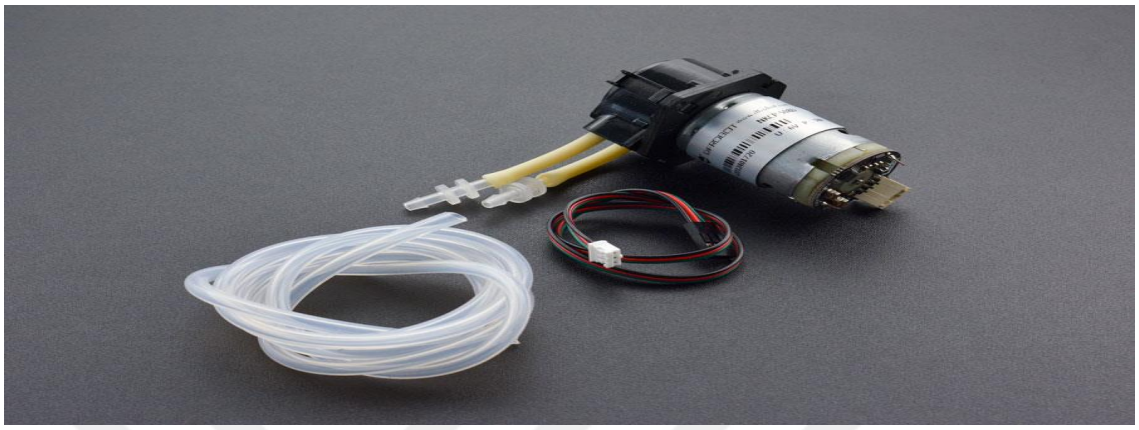

Figure 3.5. The peristaltic pump set.

Doing human trials in this stage is difficult, complicated, and not necessarily accurate due to the wide range of parameters related to the human body, not to mention the possible differences between the candidates' bodies. For those reasons, there was a need to emulate the human heart. Thus, a decision was made to create a phantom emulation of the heart-pumping mechanism, which led to the use of the peristaltic pump. As shown in figure 6. The peristaltic pump was used to represent a pumping heart with two arteries in a closed system. The different tools and materials are shown in Figure 6. Are mentioned in Table 3.1. It should be noted that there were two bottles of water in the experiment set, but only one of them was shown in Figure 3.6. Due to the size of the picture's frame.

Table 3.1. A set of tools used with the peristaltic pump with description.

Name of the material	Description
MDF wood board	A board made of wood was used to fix all the experiment tools.
Peristaltic pump	It was used to emulate the working mechanism of the heart by transferring water from one bottle to another using two tubes.
Power amplifier circuit	It delivers the required electrical power for the peristaltic pump.
Two-headed silicon tube	It was used to insert an artificial clot into the system when it was needed.
Small pieces of rubber	They were used as artificial blood clots
Two bottles of water	They hold the water that is needed to be trasfered through the system.
Piezoelectric transducer	Measures the vibrations resulting from the moving water through the tubes.
Two elastic tubes	They transfer water from one bottle to another; each tube is connected to one side of the peristaltic pump.
A set of cables	They connect the power amplifier circuit with the peristaltic pump and they also connect the power supply to the power amplifier.

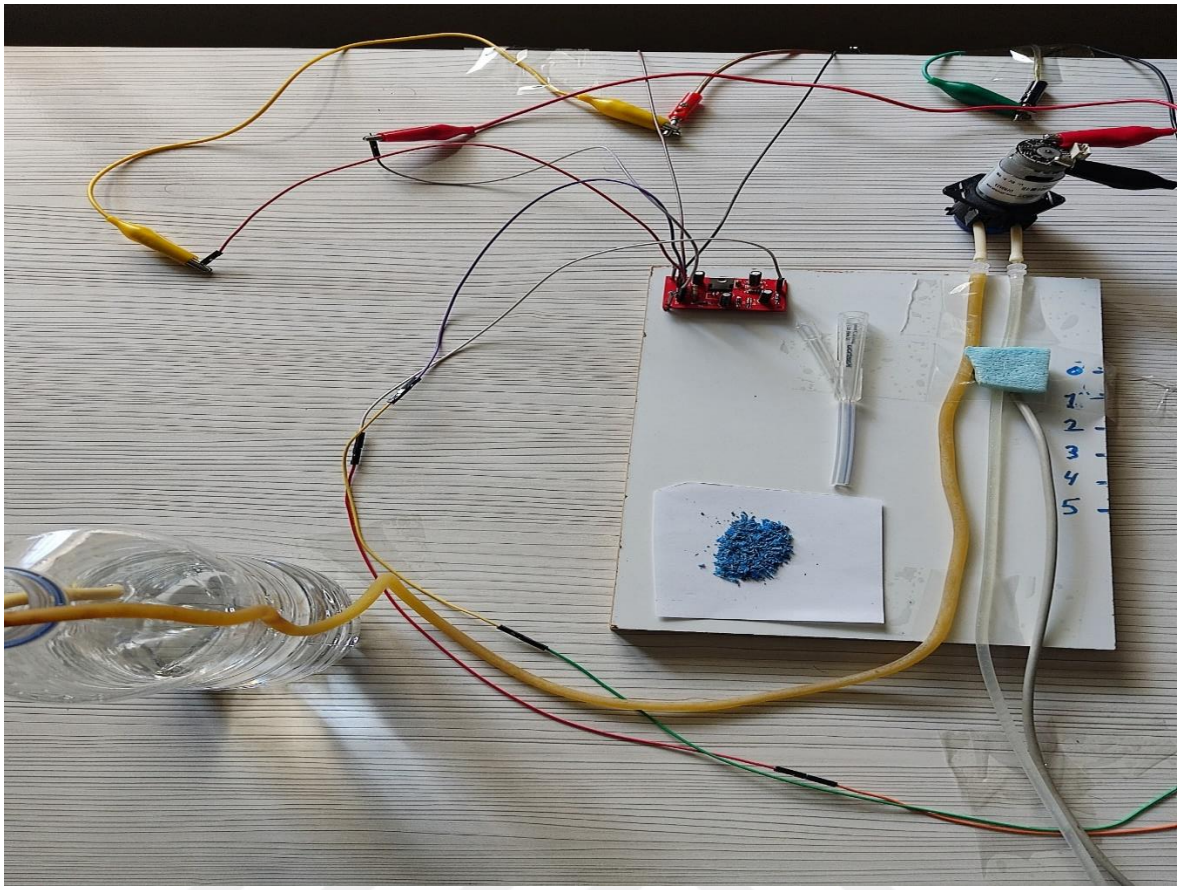

Figure 3.6. A peristaltic pump with a set of tools.

3.1.4. Power Amplifier

The LM1875 is a power amplifier that offers very low distortion and high-quality performance. It is usually used for audio applications, but in this case, it was used to power the peristaltic pump. As for the circuit configuration, as shown in Figure 3.7. The single supply configuration was chosen for this application with the removal of capacitor C6 and the speaker, as shown in Figure 3.8. The capacitor C6 was removed from the circuit so it would be possible to get the offset voltage at the output of the circuit and use it to power the peristaltic pump continuously without a stop. The speaker was replaced by the peristaltic pump.

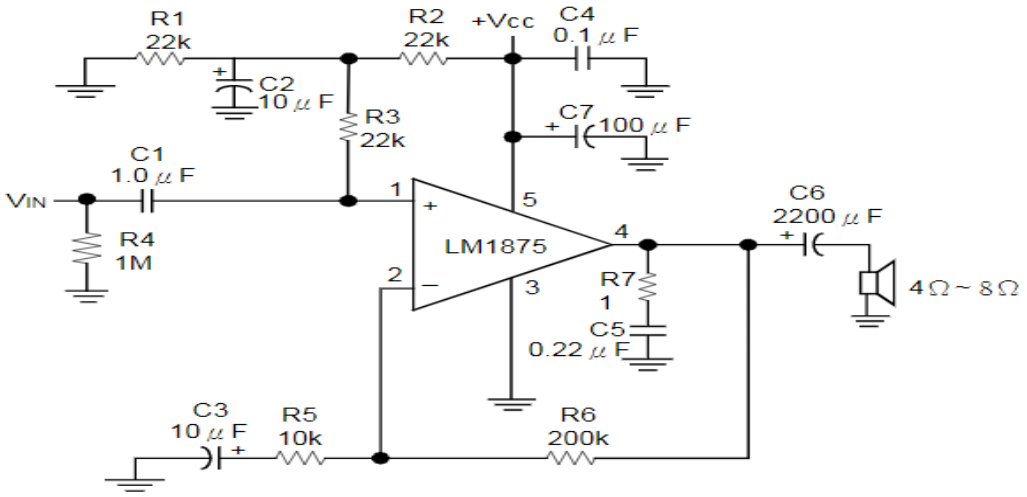

Figure 3.7. single supply configuration for the lm1875.

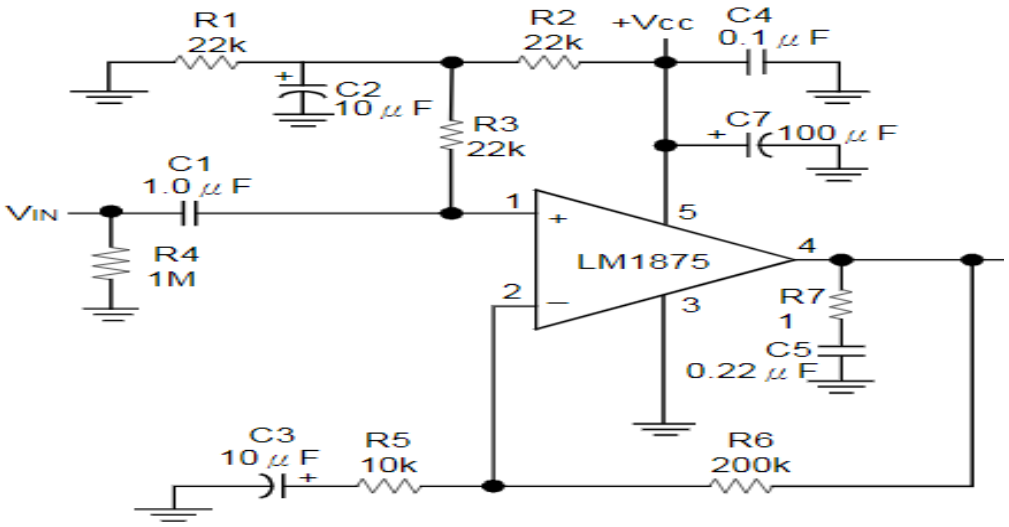

Figure 3.8. modified single supply configuration for the lm1875.

3.1.5. A Fixed Chair

While there are different axis when it comes to measuring the BCG signals, the obtained signals for each axis are not fully identical, but they are also not so different. The experiments were done using a chair and measuring the BCG signals in the anterior-posterior axis where the candidate has to sit on the chair, as shown in Figure 3.9. A piezoelectric transducer was placed on the chair's back from the inside direction, and when the candidate lays back, the back of the candidate will touch the transducer. Figure 3.10. Shows a closer look at the measurement set.

Figure 3.9. A piezoelectric transducer is placed in the inside direction of a chair.

Figure 3.10. A closer look at the measurement set.

3.1.6. TOPSFLO Pump

TOPSFLO is a small brushless pump that has the capability to pump around 5L of liquid in one minute. This pump was used as an alternative to the peristaltic pump to provide higher pressure and better flow. As shown in Figure 3.11. The pump has one input and one output, and two tubes with different diameters were connected to the pump. Also, two 5L bottles of water were used to create a water transfer system, as shown in figure 3.12. a faucet was connected to one of those bottles to add a switching mechanism to the system.

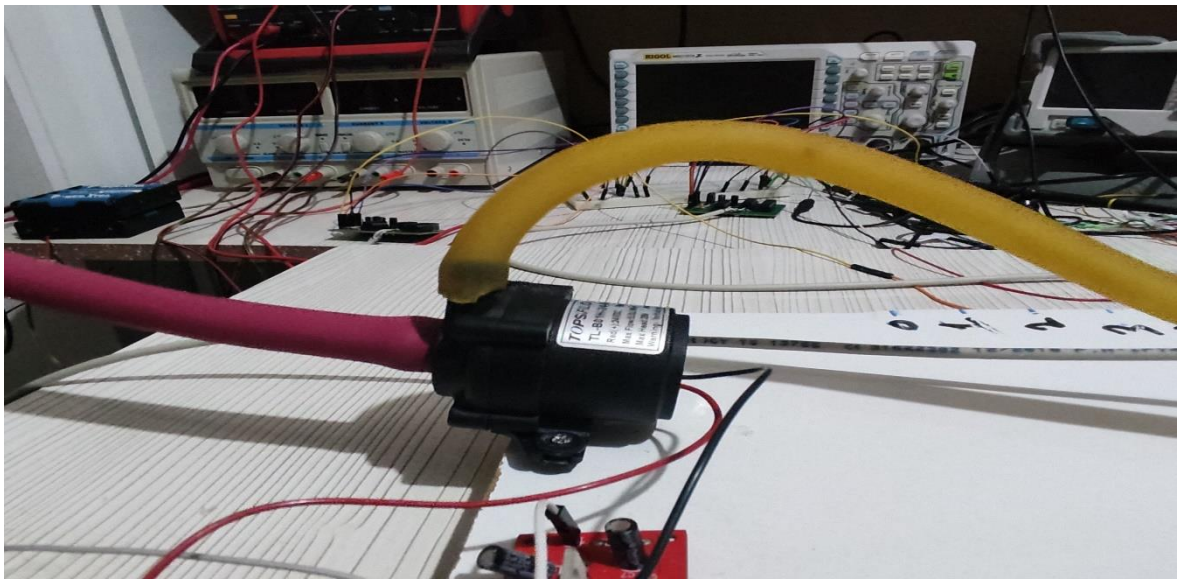

Figure 3.11. TOPSFLO Pump.

Figure 3.12. A faucet connected to 5L bottles of water.

3.1.7. Two BCG Circuits with an Arduino UNO

Two BCG circuits were used to measure alternating signals resulting from the pressure that comes from the flow of water in the elastic tubes, which will provide the necessary data that will later be used to locate the location of any potential blood clots, as shown in Figure 3.13. Each BCG board has a piezoelectric sensor, those two sensors will be placed later in two different locations to measure the pressure in the elastic tube when the water starts to flow through. As shown in Figure 3.14. an Arduino UNO was used with the BCG boards; the measured data from the BCG boards will be transferred to the Arduino so that the Arduino can read the data and transfer it to Excel software in order to generate different graphics, which will provide much help in understanding the concept of detecting blood clots.

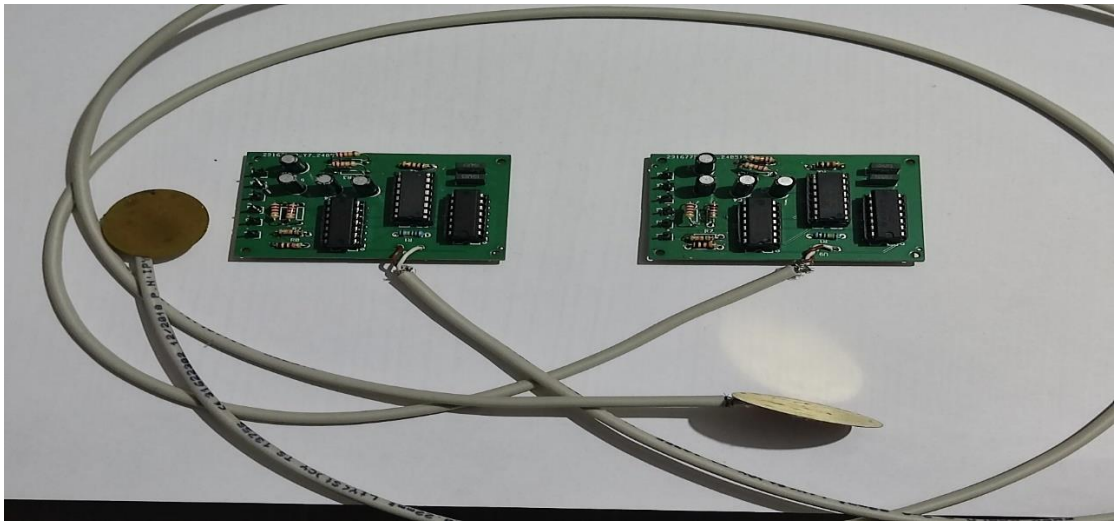

Figure 3.13. Two BCG boards

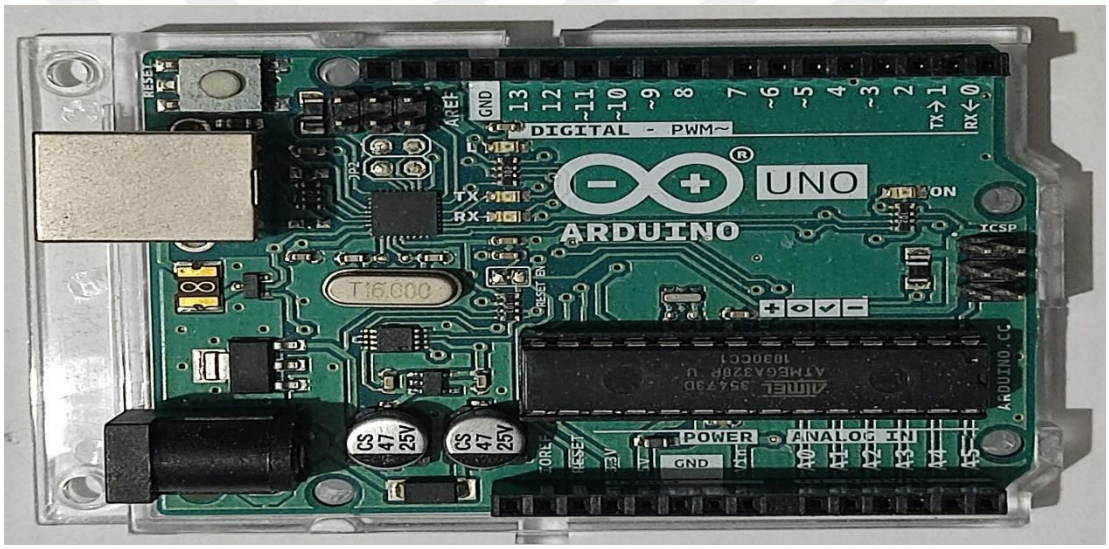

Figure 3.14. Arduino UNO

3.1.8. 3.1.8. Other Materials

Other materials were used to help create a system that delivers an artificial homemade blood clot.

As shown in Figure 3.16, small, tiny pieces of solder were obtained by melting solder wires. The solder particles would be used as an embolus later. As shown in Figure 3.15, a plastic cylinder, a T connector, and a two-headed tube were also used to deliver the solder particles into the system.

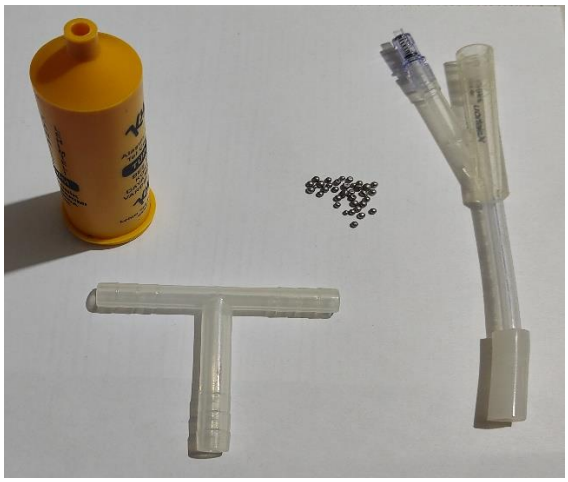

Figure 3. 15. Other Materials

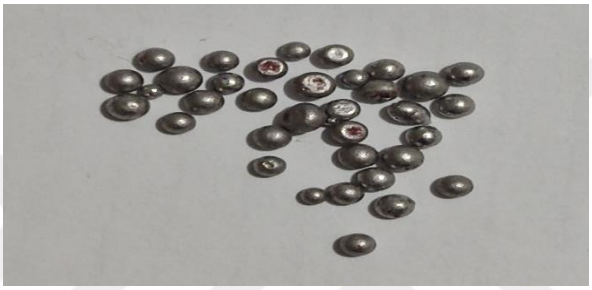

Figure 3. 16. solder particles

Fake blood, which is usually used for makeup, was used in combination with glue to create an artificial blood clot. The artificial blood would be glued to the inner walls of the elastic tube so it could represent a real blood clot. Figure 3.17 shows a fake blood substance and a sample of an obstructed tube due to an artificial blood clot.

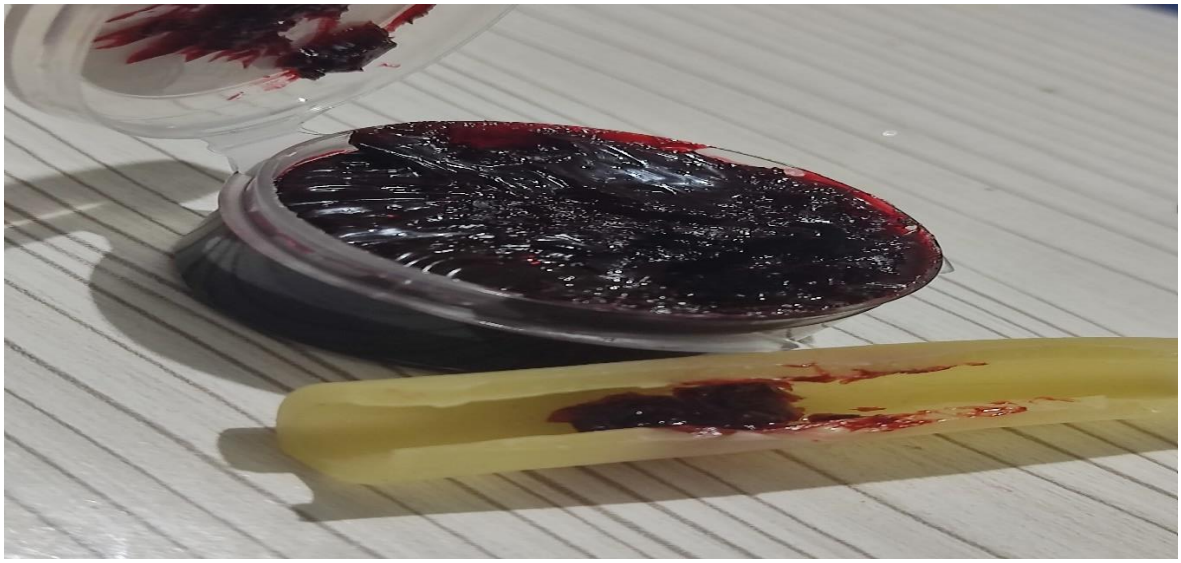

Figure 3.17. Artificial blood clot

3.2. Method

3.2.1. Block Diagram

In this work, we show two different block diagrams. The first one is the ideal block diagram that we aim to achieve, which is the ideal diagram. The second one is the block diagram of the phantom system, which we use to demonstrate the working principle of this system. Figure 3.18 and Figure 3.19 show the ideal block diagram and the phantom block diagram, respectively.

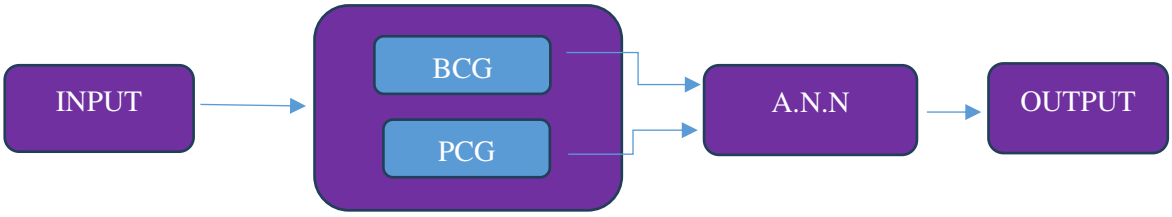

Figure 3.18. The Ideal Block Diagram.

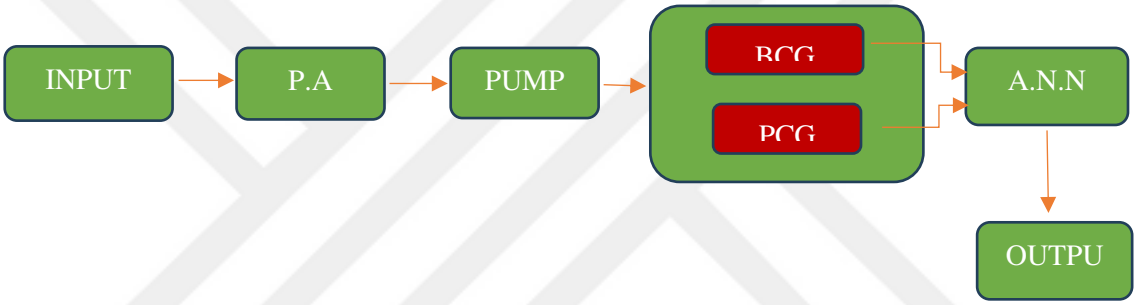

Figure 3.19. The Phantom Block Diagram.

As mentioned before, the focus of this work will be on the phantom system. The first block of the phantom system is the input block; here, at first, an artificial signal with an amplitude of 1V and frequency of 1 Hz was provided from a signal generator and given as an input for the phantom system, as shown in Figure 3.20. Later, the signal from the signal generator was replaced by a real BCG signal. The BCG signal was obtained from a BCG PCG detecting circuit, as shown in Figure 3.21. The second block is the power amplifier block. This block receives the input signal, amplifies its power, and forwards it to the next block, which is the pump block. In the pump block, the pump would work according to the given input signal, which can be a sine wave or a BCG signal. In the next block, the core of the system is represented by the circuit that measures both the BCG and PCG signals of the pump; then, the BCG and PCG signals would be fed to the block of A.N.N to train the artificial neural network and get a classification of normal and non-normal signals.

It should be pointed out that the block of the BCG and PCG signals is identical to the input block of the system; in other words, a BCG signal is given to turn on the pump. When measuring the output of the pump, the obtained output signal should be similar to the input signal. After testing the phantom system and making sure that it's working properly, an artificial clot would be inserted in

the tube of the suction side of the pump. At the end a distortion in the output signal of the pump should be observed. If the distortion happens that would imply that the system is successful.

Figure 3.20. Providing the input signal from a signal generator.

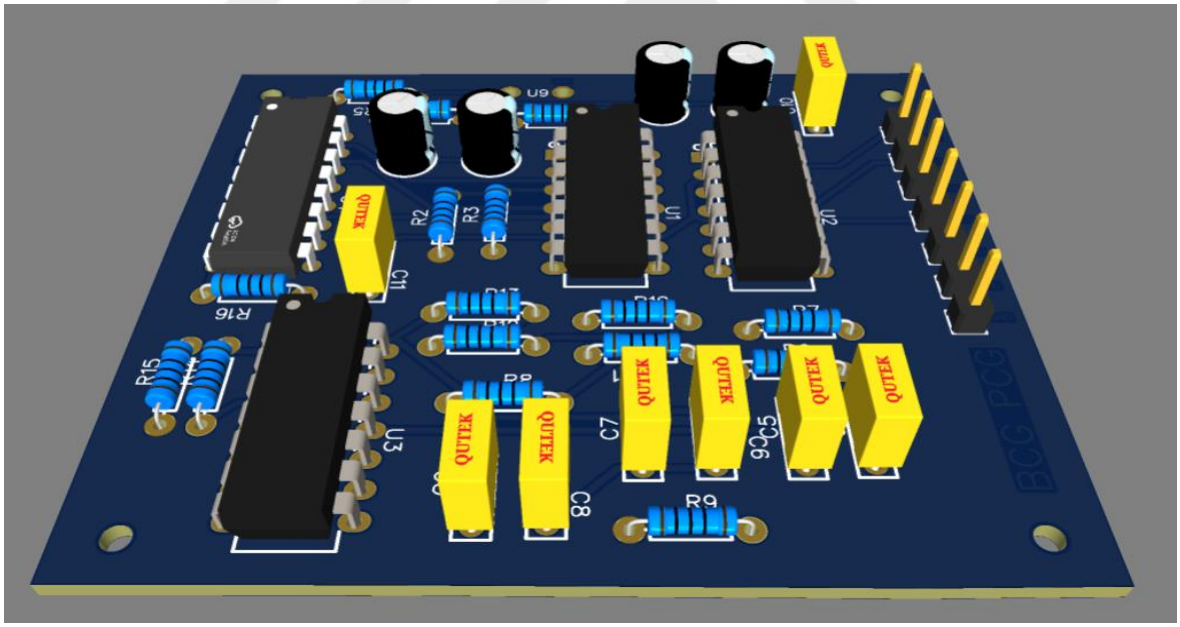

Figure 3.21. BCG PCG detecting circuit.

3.2.2. Butterworth Filter

A filter is a system that allows the wanted frequencies to pass through while it blocks the unwanted signals. Filters are usually used to reject noise signals and denoise the main signal so it can be processed later without the unnecessary noise signals. There are many filter configurations, each has its purpose. Since the Butterworth filter has a very flat frequency response it has been chosen for this work as the best filter. A Butterworth filter has -40db/decade roll off past of cutoff frequency.

As shown in Figure 3.22. A band-pass Butterworth filter was used as an essential and critical part of the circuit.

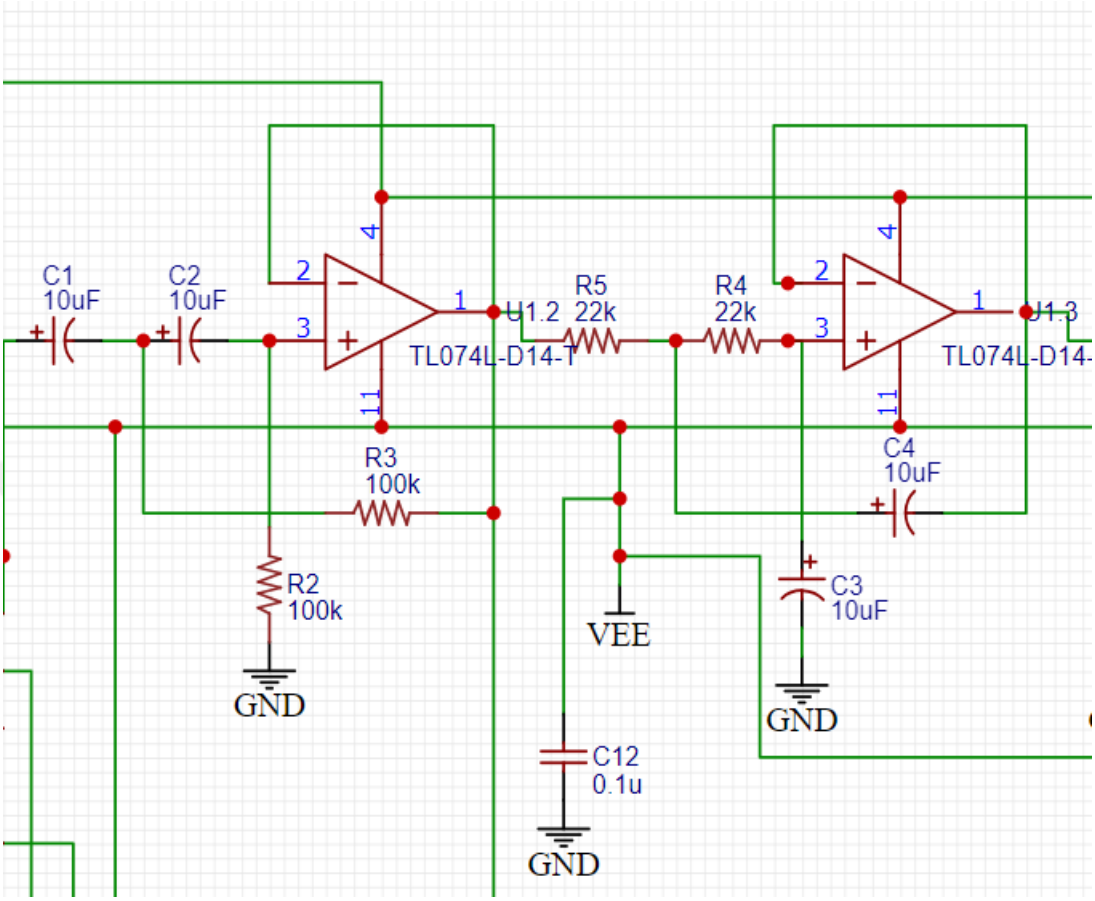

Figure 3.22. A Band-Pass Butterworth filter Circuit.

3.2.3. Circuits

As was explained in the previous sections, an LM1875 power amplifier circuit and a BCG and PCG detection circuit were used in this work. The circuits were designed using the online platform Easy EDA. As for the BCG PCG circuit, it consists of two parallel circuits. One is responsible for detecting the BCG signal, and the other is responsible for detecting the PCG signal; both of these circuits share the same input stage. Figures 3.23. And figure 3.24. show the schematic of the power amplifier circuit and the PCB layout for the BCG PCG circuit respectively. Figure 3.25. Shows the block diagram of the parallel circuits.

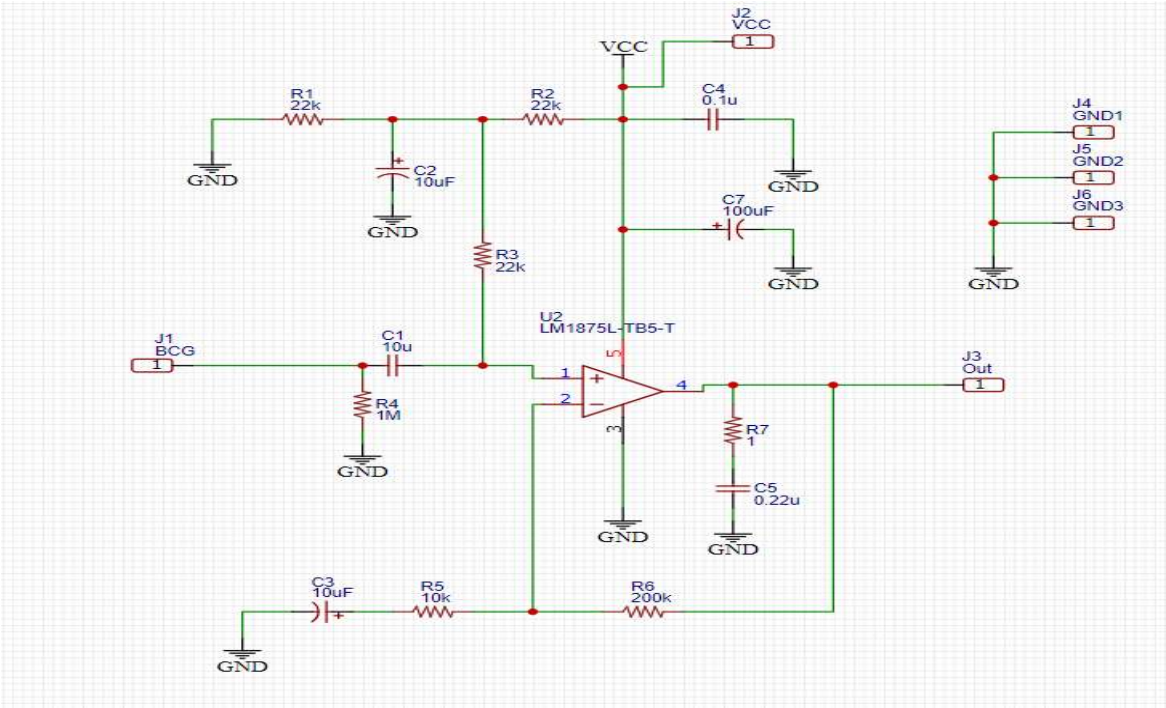

Figure 3.23. A 3D PCB Of The Power Amplifier LM1875 Circuit Schematic.

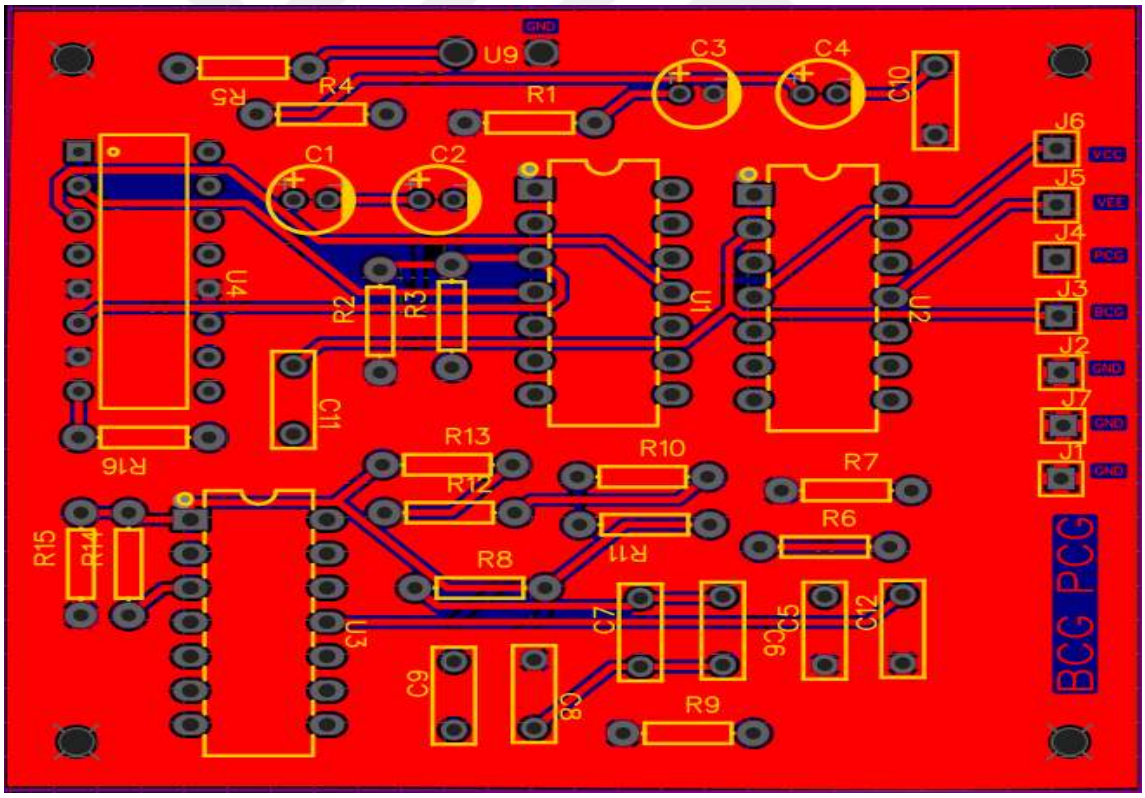

Figure 3.24. BCG And PCG Detection Circuit PCB layout.

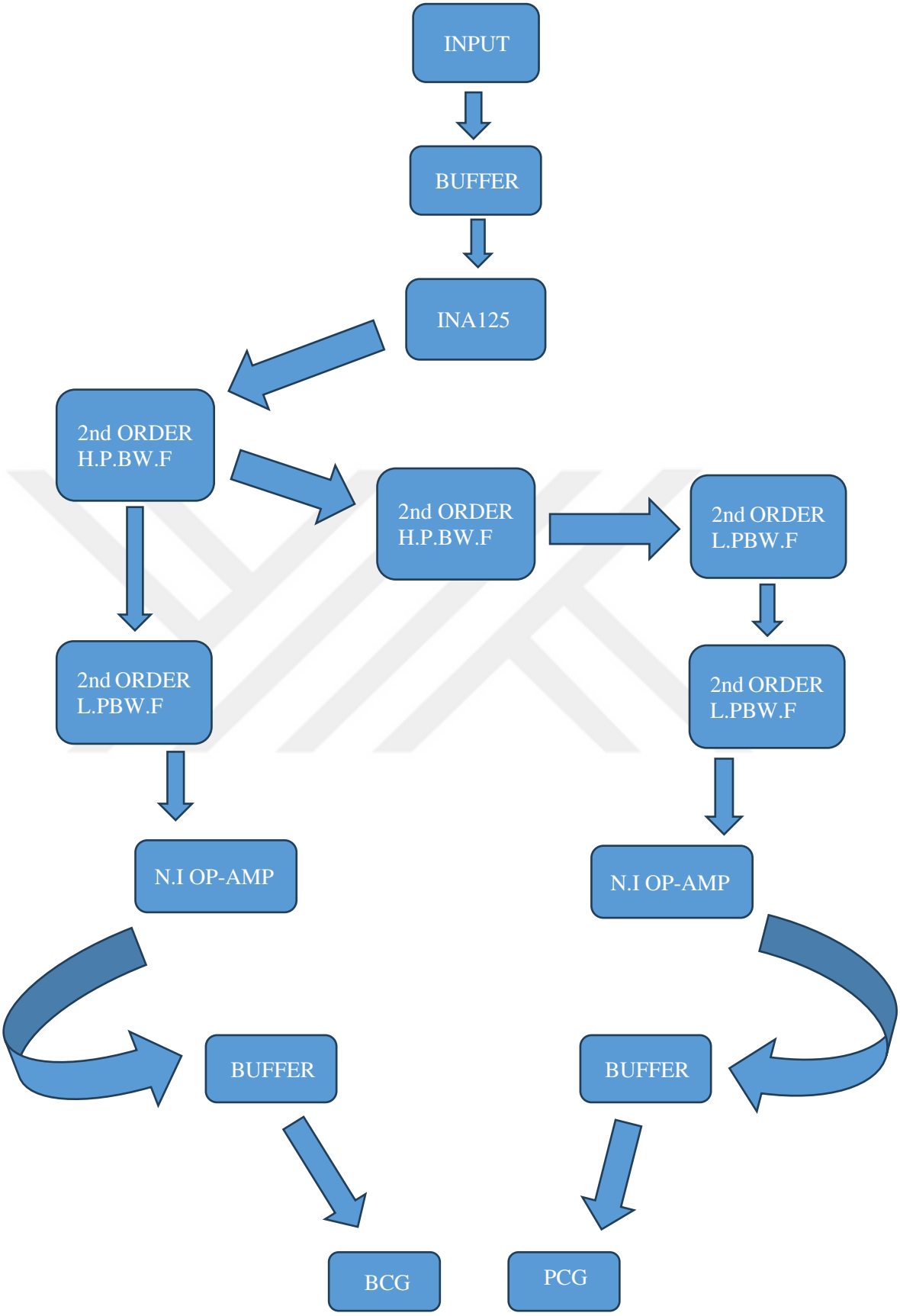

Figure 3.25. The Block Diagram of the parallel BCG and PCG circuits.

3.2.4. Multilayer Perceptron (MLP)

Multilayer perceptron is a fully connected feed-forward artificial neural network with at least 3 layers: input, output, and at least one hidden layer. The multilayer perceptron consists of many neurons with a non-linear activation function. The MLP was used in this work and trained with the measured BCG and PCG that represent normal signals so that the MLP can detect any errors or distortion in the BCG and PCG signals. Thus, the device will be able to tell if there is a blood clot or not in the candidate's body. The MLP structure is shown in Figure 3.26. With input layer, hidden layer. And output layer in blue, yellow, and red respectively.

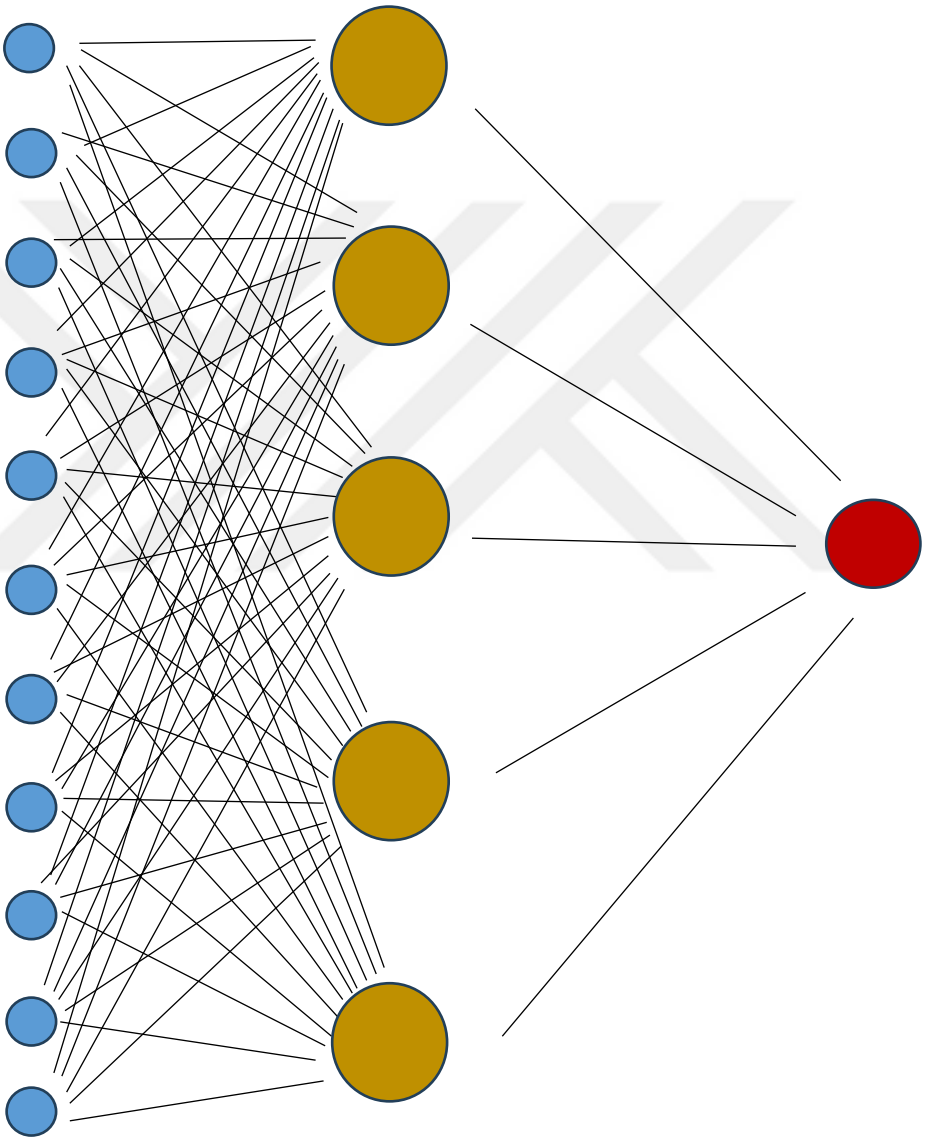

Figure 3.26. A Multilayer Perceptron Structure.

4. RESULTS AND DISCUSSIONS

4.1. BCG Results

As it was discussed before, the Ballistocardiogram is a measure of the ballistic forces caused by the cardiac ejection of blood, in other words it is the measurement of the blood vessels' reaction or vibration to the blood flow that goes through those vessels. As it shown in figure 4.1. the BCG signal consists of different waves. The names and the definition of these waves are shown in table 4.1.

Table 4.1. Names of BCG waves and functions.

Name of the wave	Wave's function
G wave	A pre-systolic wave is related to events that occur before the systolic phase.
H wave	Occurs with the atrial contraction.
I and J waves	I wave occurs in the early systolic phase while J wave occurs late in the systolic phase, they are associated with the injection of blood in the aorta and other large vessels.
K and L waves	They represent a reflection of the pressure at the peripheral vessels
Other waves	Waves like the M and N waves occur during the diastolic phase, and they represent oscillations caused by the blood flow and vessels vibrations.

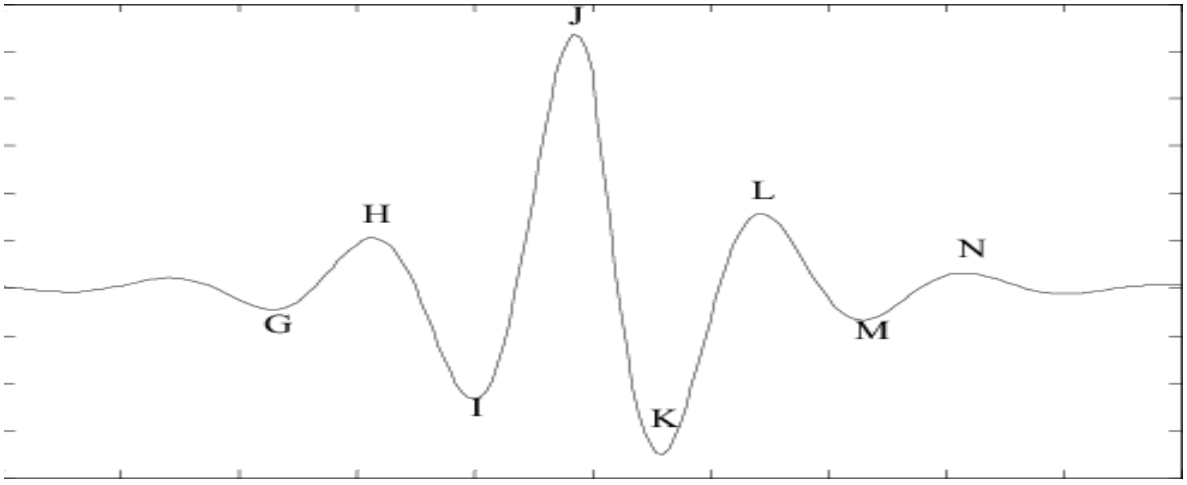

Figure 4.1. The BCG signal waveform.

As for the obtained BCG signals from this work, the BCG signals were captured successfully and after passing the signals through the different stages of the BCG circuit from amplifiers and

filters, the output signals were seen clearly on the screen of the oscilloscope, the oscilloscope shows the amplitude, time, frequency and other parameters of the mentioned signals, it was noticed that the obtained signals consist of the G,H,I,J,K and L waves which represent pre-systolic, systolic and diastolic phases of the cardiac cycle. The N wave was the only absence wave, which basically represent oscillations and vibrations. This BCG signal was used in the next stage as an input signal to the power amplifier circuit to make the peristaltic pump work similarly to the real human heart. Figure 4.2. Shows the obtained BCG signal and its waves on the oscilloscope screen.

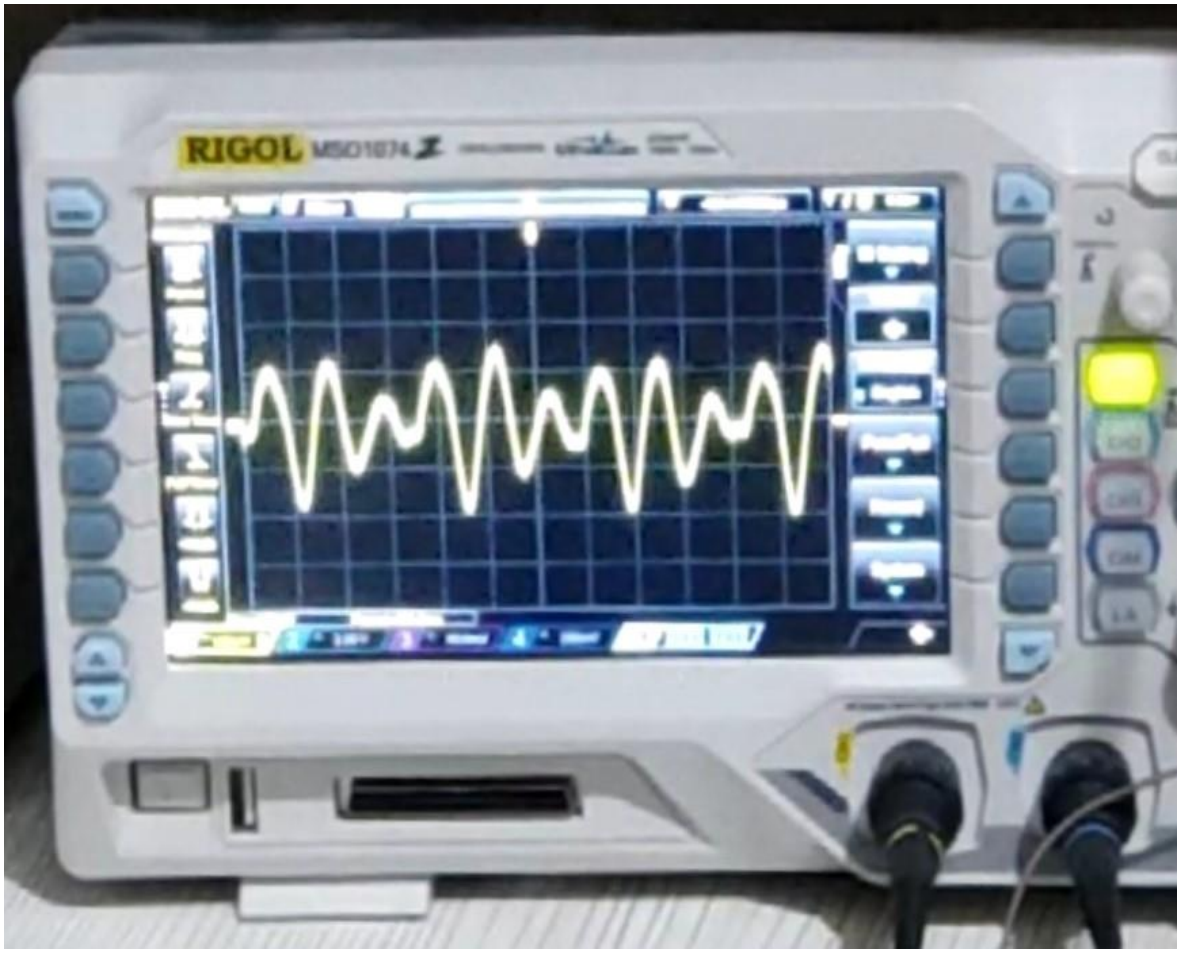

Figure 4.2. The BCG signal and its waves are shown on the screen of the oscilloscope.

While the BCG signal is going to be used as an input for the next stage of the system, the recording function of the oscilloscope is used to capture the BCG signals and transfer them to a USB, which will be later on connected to a computer to transfer the collected BCG data to MATLAB. The transferred data to MATLAB will be used to train the Artificial neural network configuration so it can tell the difference between a clean BCG signal and any other BCG signals that has errors or distortion.

4.2. PCG Results

The phonocardiogram is the recording of the sounds and murmurs made by the heart. With every heartbeat, blood flows through the vessels, the heart valves open and close, the opening and closing of the heart valves, and the acceleration and deacceleration of the blood make sounds. Measuring those sounds gives a lot of valuable information regarding the heart's condition, and it can detect problems and issues within the heart or the vessels if there are any. There are two main sounds of the heart, S1 and S2, which occur during the systolic and diastolic cycles, respectively. S1 and S2 are also called the LUB DUB sounds, which are the easiest to identify when listening to heart sounds. There are also two more sounds S3 and S4. Some healthy people have those sounds, but most of the time, when S3 and S4 are being detected, it means that there is a problem somewhere. Table 4.2. It shows the categorization of the main heart sounds, their meanings, and the cardiac phase of each sound. There are also some other sounds called heart murmurs, which are whooshing, blowing, or rasping sounds when turbulent blood flows through the heart valves. It can also happen when blood flows in a backward direction instead of a forward direction. It should be noted that murmurs can happen during both systolic and diastolic cardiac phases, whereas systolic murmurs occur during heart contraction and diastolic murmurs occur during the relaxation phase.

Table 4.2. The main sounds of the heart.

Heart Sound	Meaning	Cardiac phase
S1	Occurs when the AV valves close.	Systolic phase
S2	Occurs when the Semilunar valves close.	Diastole phase
S3	Refers to the flowing of blood into the ventricles.	Diastole phase
S4	Refers to atrial contraction	Diastole phase
Heart Murmurs	Abnormal sounds	Both the systolic and diastolic phase

There are four main locations on the chest to measure the heart sounds. Those locations are aortic area, pulmonary area, mitral area, and tricuspid area. Each sound of the four main sounds can be heard louder or lower than the other sounds depending on the location of the measurement. In this

work, the PCG signals were measured in the tricuspid area where S1 can be seen and heard clearly. Figure 4.3. Shows the ideal PCG signals.

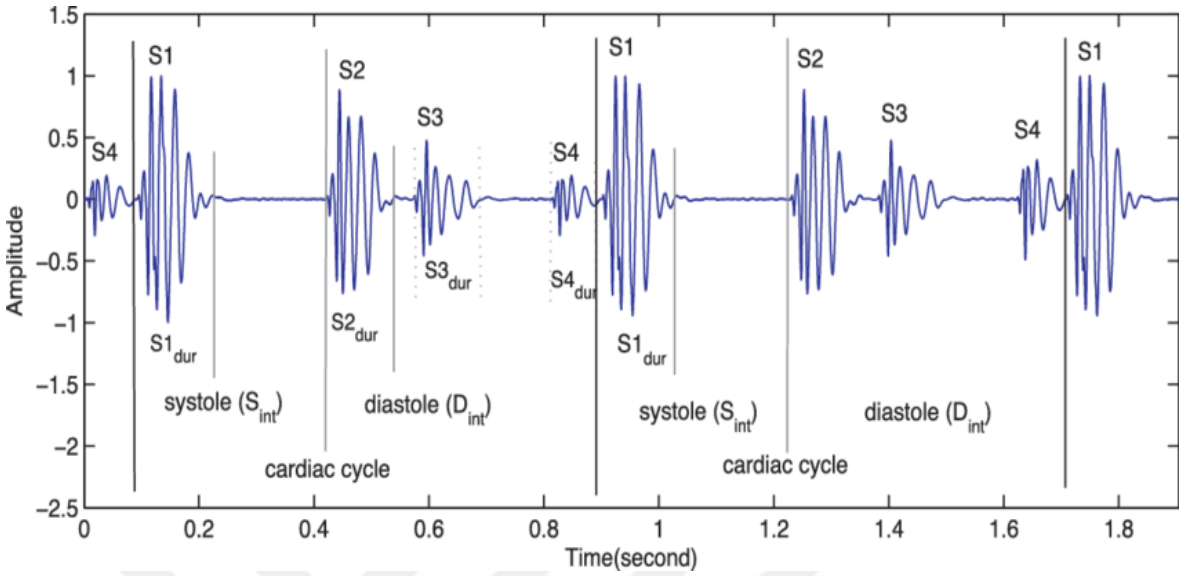

Figure 4.3. The main sounds of the heart.

In the laboratory PCG signals were measured and shown on the screen of the oscilloscope. The PCG signals were measured in two different ways. At first, the piezoelectric transducer was placed on the chest to see whether it would detect the vibrations in the chest or not. The results from the first measurement can be seen in Figure 4.4.

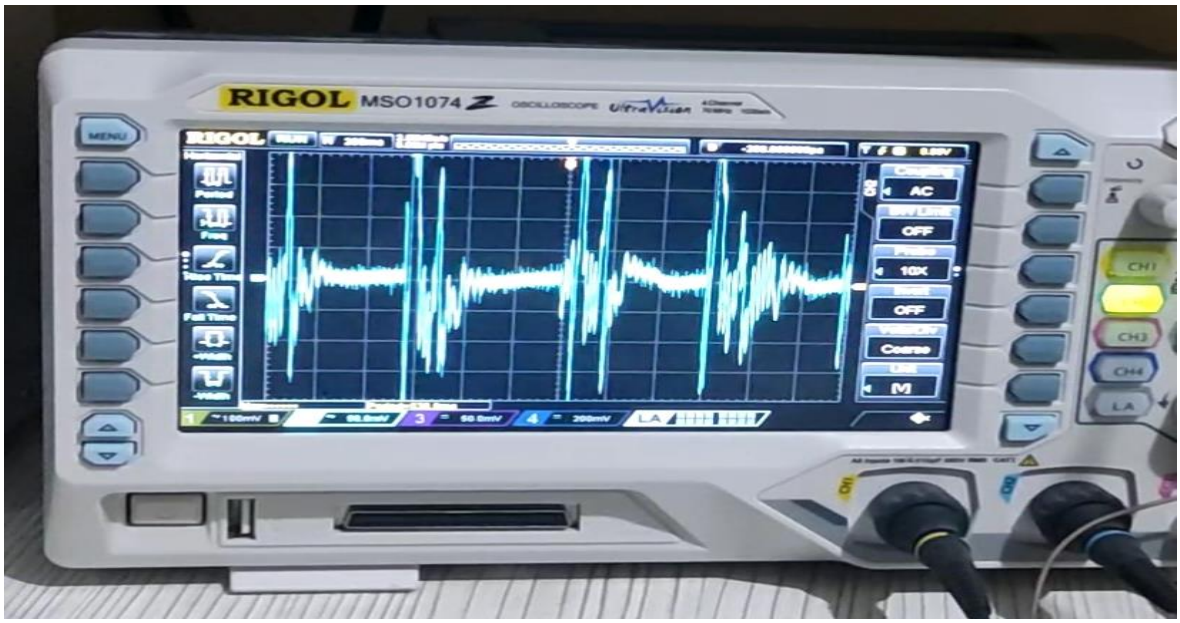

Figure 4.4. The PCG signals shown on the screen of the oscilloscope.

It is clearly seen that the obtained PCG signals from the first measurement have two main sound waves, S1 and S2, which correspond to the systolic and diastolic cardiac phases, respectively.

In the second measurement which is the main and important one, the piezoelectric transducer was placed on the inside face of the chair so it can make contact with the back of the candidate's back. The problem is when the candidate sets back to make contact with the transducer, and because the candidate is putting pressure on the transducer, the transducer will keep generating a continuous distorted signal interacting with the real PCG signals, as shown in Figure 4.5. Because of that, it will not be possible to get data from the PCG signals and transfer it to MATLAB to train the neural network. However, the neural network will be trained with the BCG signals.

Figure 4.5. The second PCG measurement shows the distortion.

The filtering methods used in this work didn't help with the distortion that was seen in the second measurement. Even though the PCG signals in the second measurement were distorted, it was still possible to identify S1 and S2, thus being able to tell whether there was a problem or issue with the heart or not. The results can differ from one person to another depending on the thickness of the skin thickness of the fat layer, heartbeat amplitude, and other factors. Even within the same person, the measurements can show different results between morning and evening measurements, or it can also differ depending on the temperature of the environment. The obtained PCG signals from the first and the second measurements weren't converted to sounds. They were only shown as graphics.

4.3. The Phantom experiment setup and results

After measuring each signal separately and independently of the whole system, turning on the power amplifier, and testing the peristaltic pump system, it was time to assemble all the parts together. The assembling was done in multiple steps. The first step was to get the measured BCG signal from the main circuit and forward it to the power amplifier circuit, which will power the peristaltic pump, as shown in Figure 4.6.

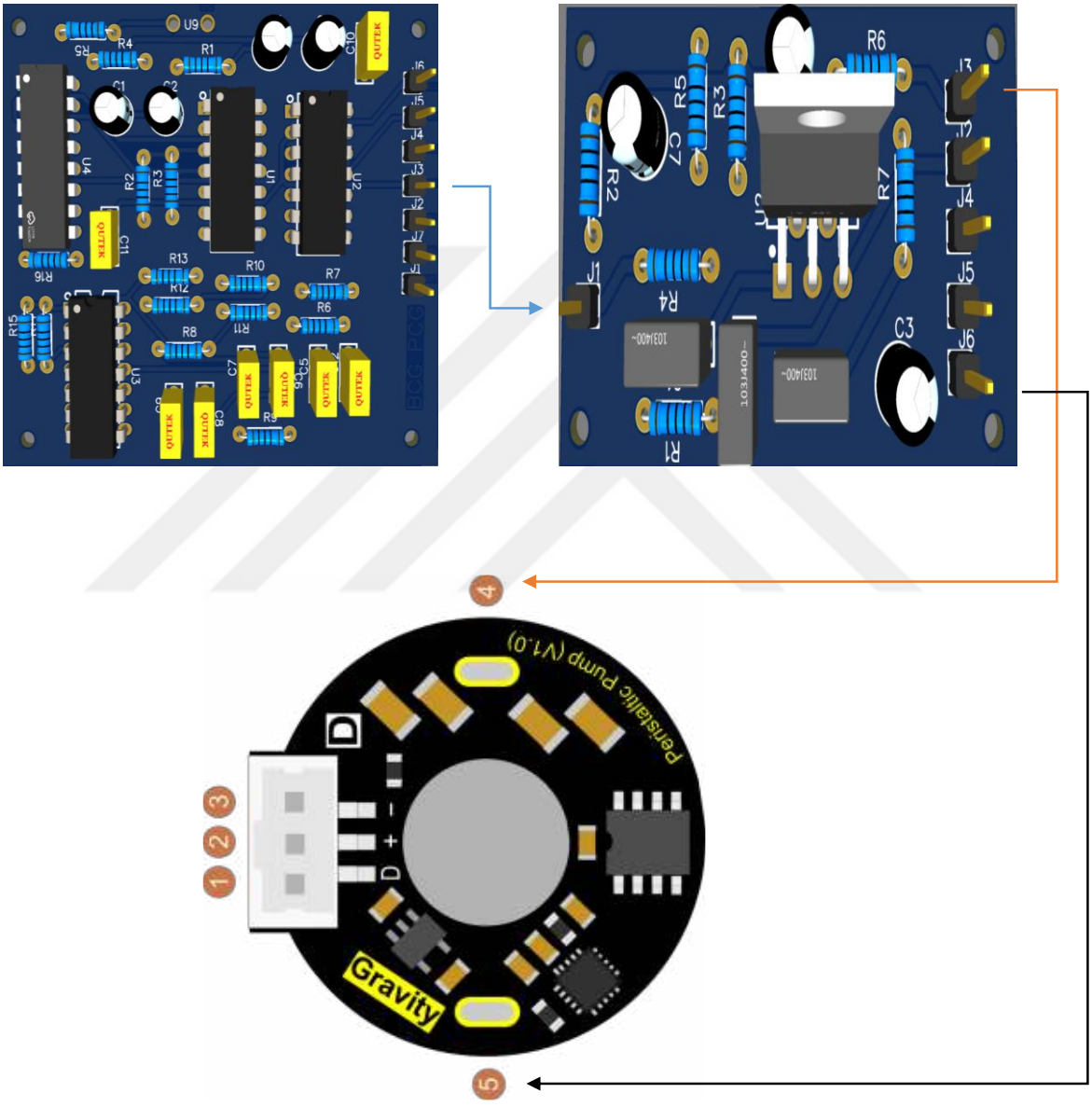

Figure 4.6. The first step of the assembled phantom system.

After assembling the circuits with the pump, the pump was tested with no problems or errors; another BCG circuit was used to measure the artificial BCG signal that resulted from the pressure of the water flowing through the tubes. In the next step the measured BCG signal from the first circuit was recorded and transferred to a computer for further processing in order to transfer the recorded signal to a function generator. Instead of continuously measuring the BCG signal the function

generator would generate a stable signal. Two oscilloscopes were connected in parallel to the output of the BCG circuit as the BCG was captured, as shown in Figure 4.7. And figure 4.8.

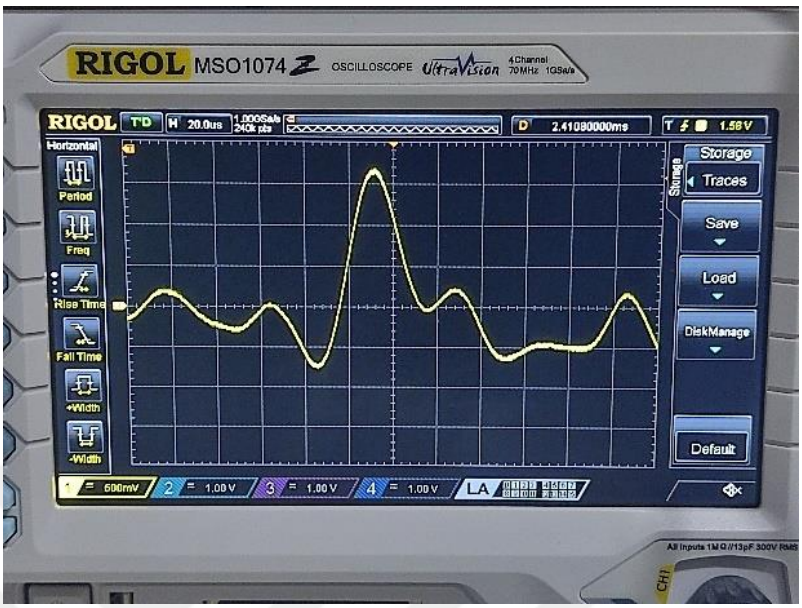

Figure 4.7. BCG from oscilloscope

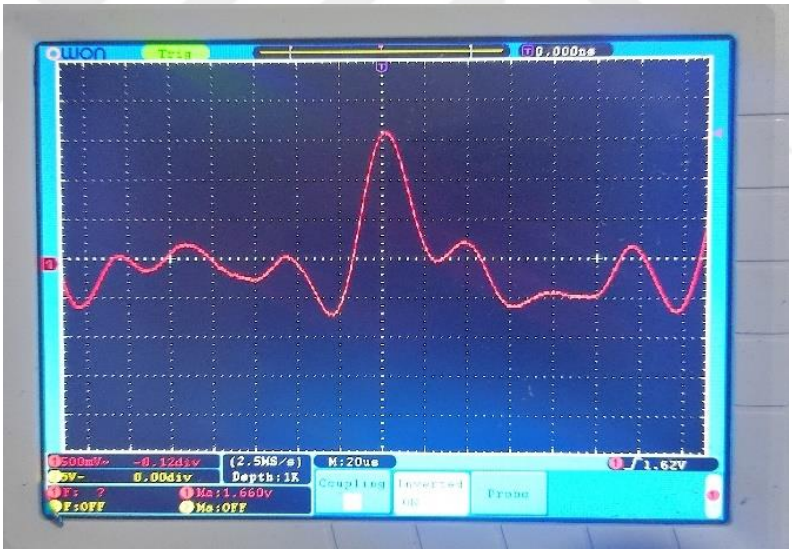

Figure 4. 8. BCG from oscilloscope 2.

The first oscilloscope was used to control the signal, while the second oscilloscope was used to record the BCG signal, the recorded signal shown in figure 4.9. Was saved as a CSV file. The CSV file was saved on a memory stick and transferred to a computer where it was opened in both RIGOL software and MATLAB software, respectively; the BCG signal was plotted as shown in figure 4.10.

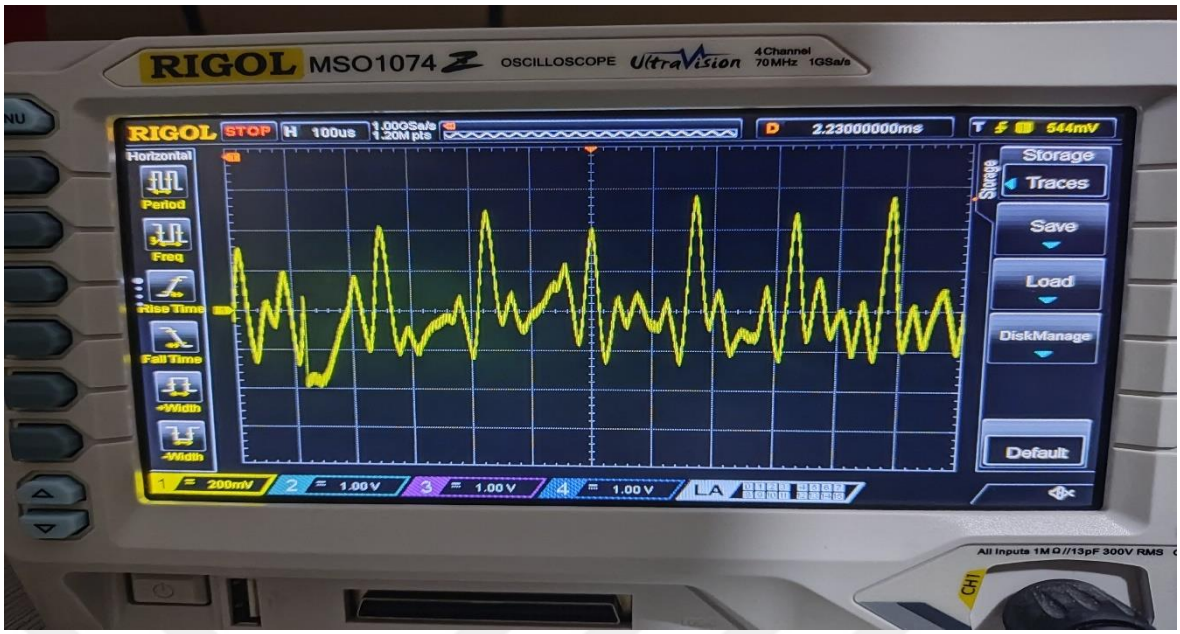

Figure 4.9. The recorded BCG signals.

Figure 4.10. The plotted BCG signals in MATLAB and RIGOL software.

The saved BCG signal was converted from the extension .CSV to the extension. RAF, later on the .RAF file was transferred to the function generator through the memory stick as shown in figure 4.11.

Figure 4.11. The transferred and converted BCG signal in the function generator.

This step was completed successfully as the function generator generates the BCG signal and forwards it to the power amplifier circuit, the power amplifier circuit on its turn powers up the peristaltic pump as shown in figure 4.12.

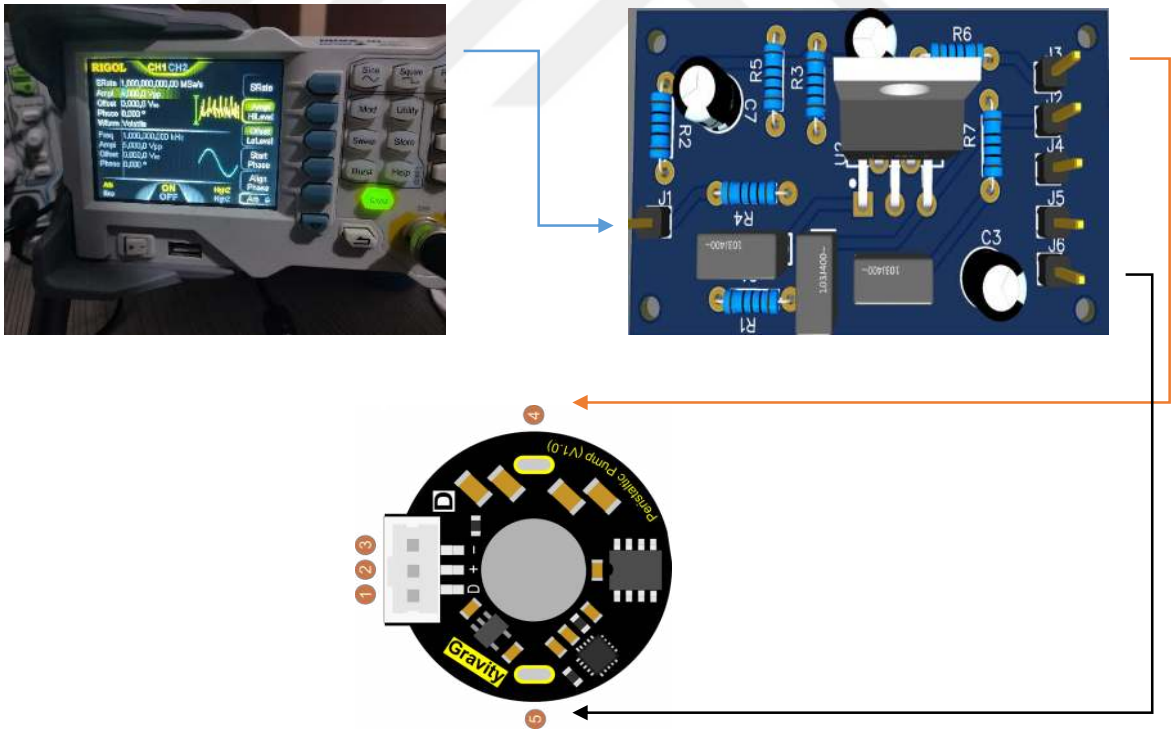

Figure 4.12. The second step of the assembled phantom system.

After assembling all the parts together, a blood detector system was established, as shown in Figure 4.13.

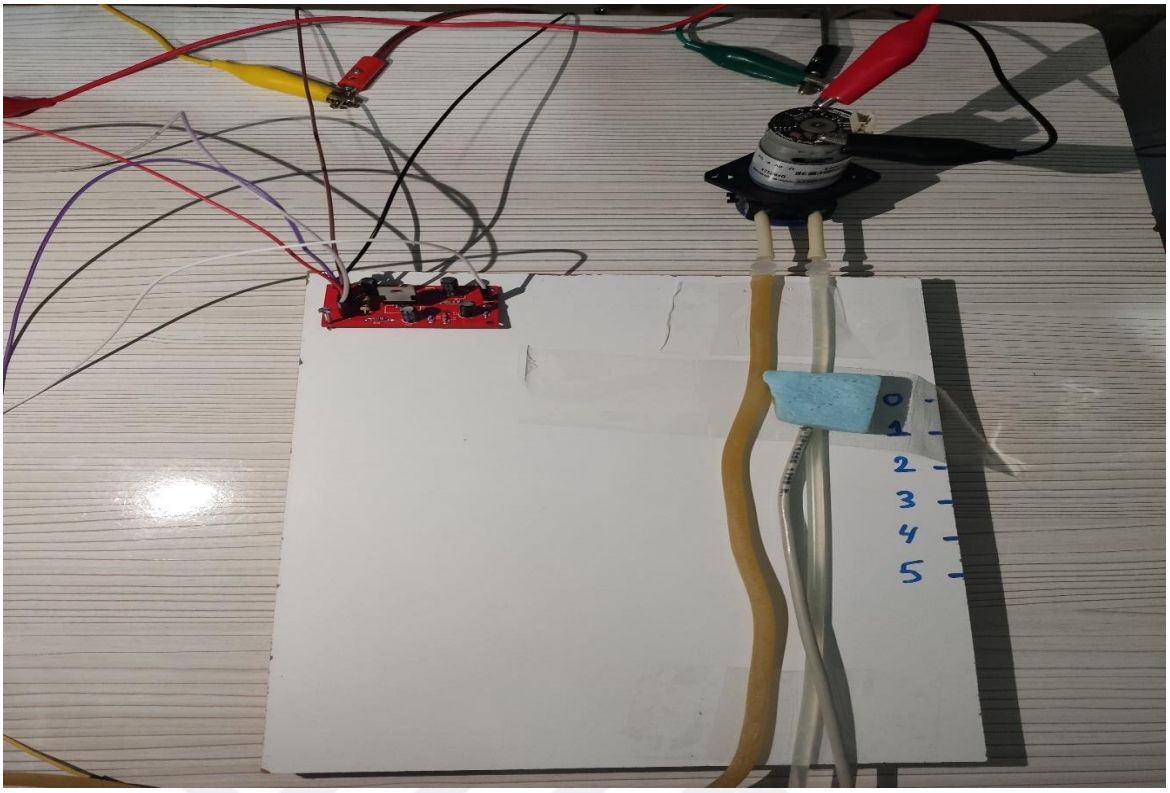

Figure 4. 13. The established blood detector system.

In this experiment, six locations were defined on the MDF wooden board. There are two centimeters between each location and the other. The piezoelectric transducer was fixed to location number zero. The purpose of this experiment was to send an artificial clot through the tube of the peristaltic pump and to capture the signal on the oscilloscope when the clot passes from each one of those locations, so in total, six graphics would be captured and saved for further processing. The six captured graphics were transferred to a computer and processed in the software RIGOL, where each signal was smoothed and filtered. The result graphics are shown below in sequence, starting with location zero and ending with location six in Figure 4.14., figure 4.15., figure 4.16., figure 4.17., and figure 4.18. And figure 4.19. respectively. The numerical results are shown in table 4.3.

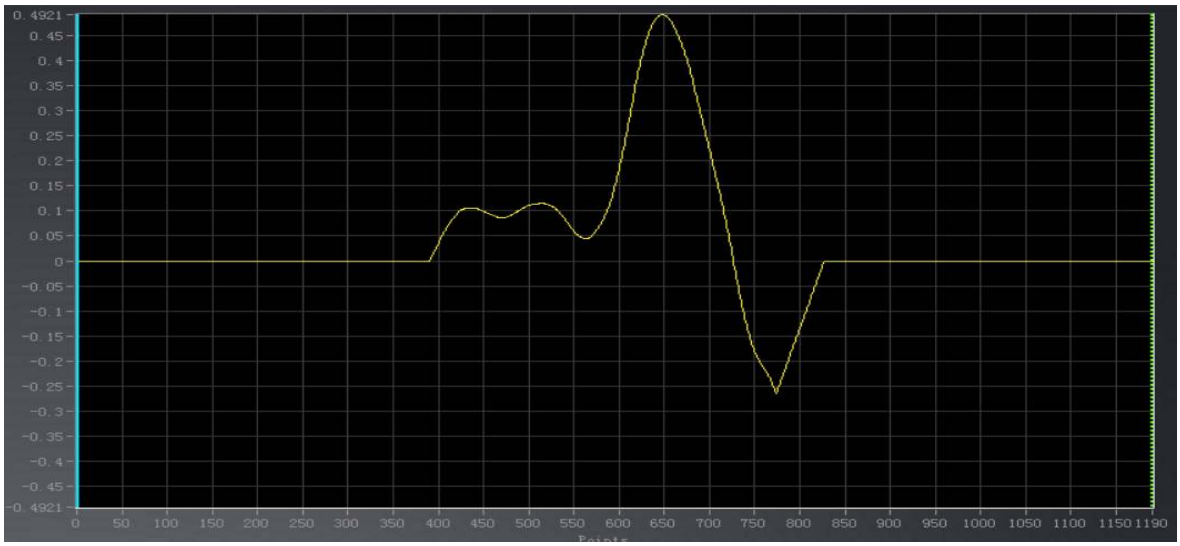

Figure 4. 14. The captured BCG signal from location zero.

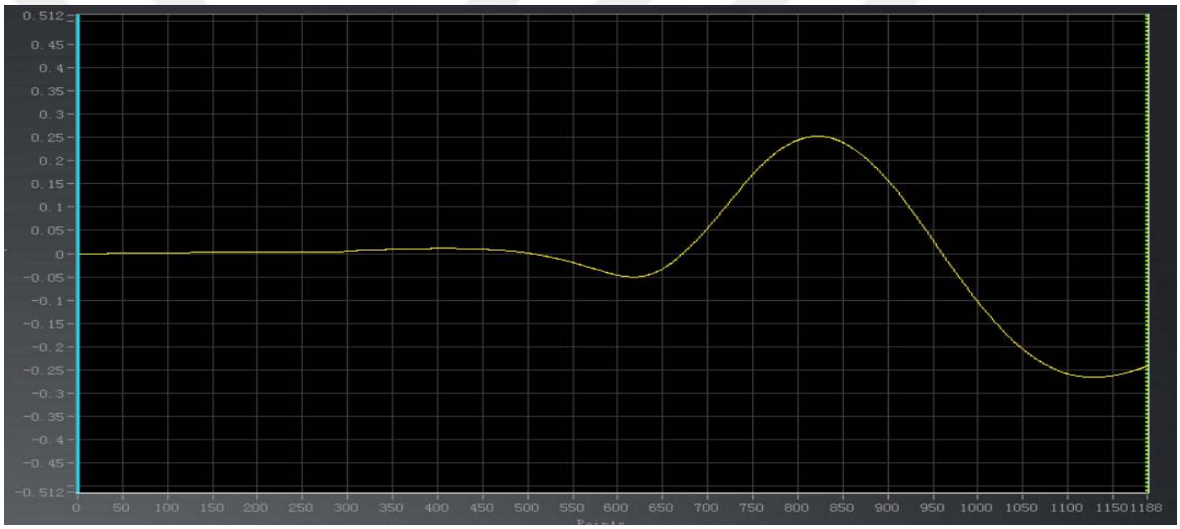

Figure 4. 15. The captured BCG signal from location one.

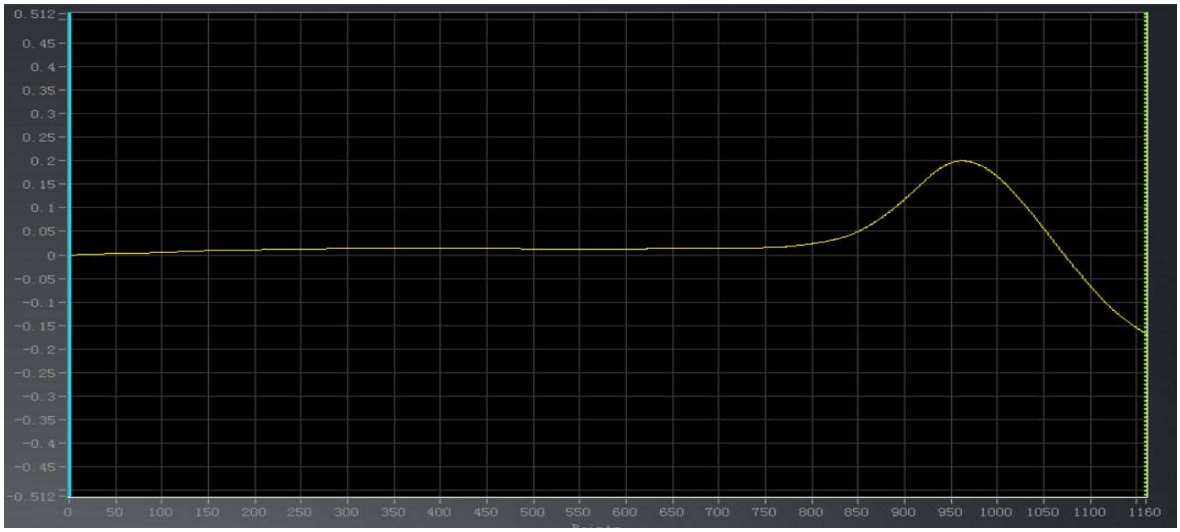

Figure 4. 16. The captured BCG signal from location two.

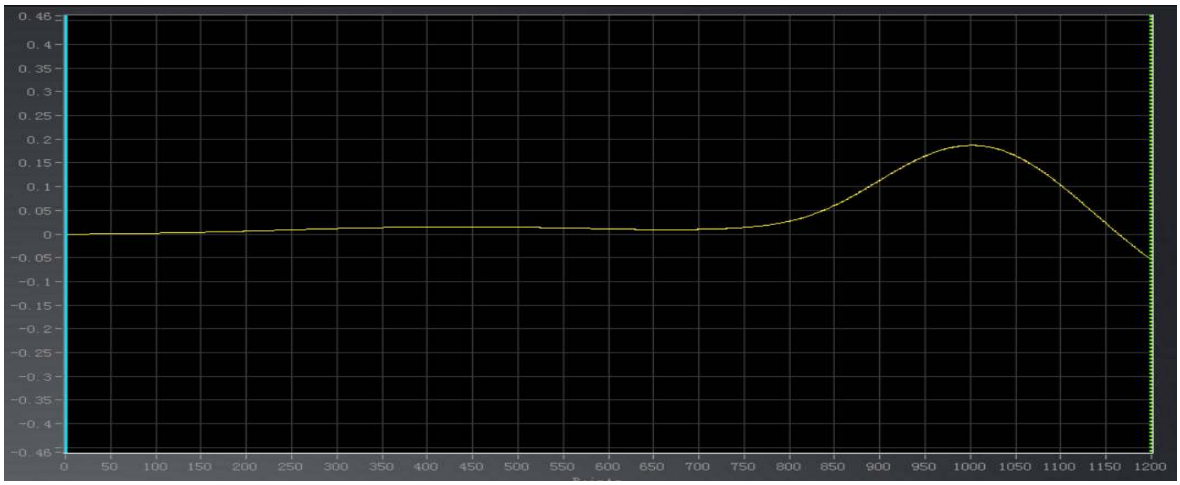

Figure 4.17. The captured BCG signal from location three.

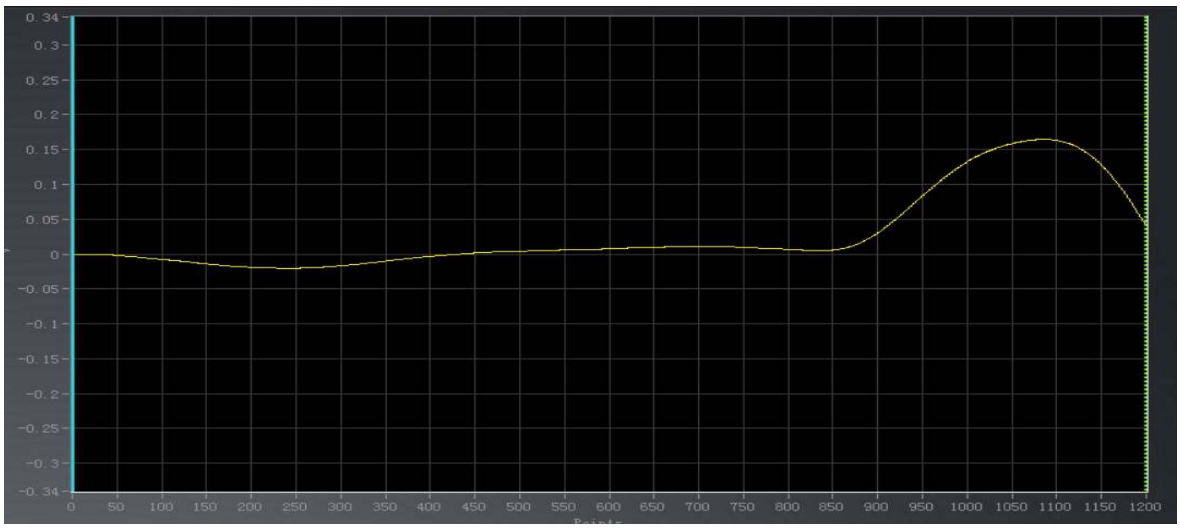

Figure 4.18. The captured BCG signal from location four.

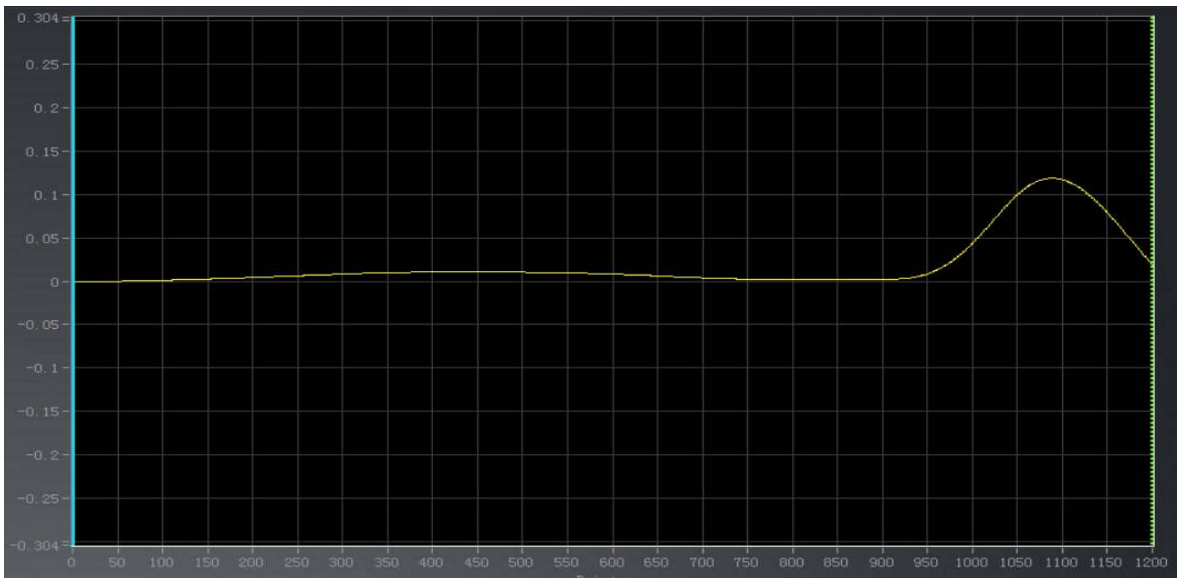

Figure 4.19. The captured BCG signal from location five.

Table 4.3. The amplitudes and peak locations of the six measurement points

Location	Amplitude	Peak Location
Location 0	0.5	650
Location 1	0.25	800
Location 2	0.2	950
Location 3	0.17	1000
Location 4	0.15	1050
Location 5	0.12	1100

It was noticed that the captured signal from location zero was losing its amplitude and shifting while the clot was flowing through the five other locations. The obtained data from the captured signals were used as inputs for the artificial neural network as it was explained in the previous sections. Using MATLAB software, a comparison between a normal BCG signal without a clot generated from the peristaltic pump and each signal captured from the six different locations was made. The original BCG signal from the pump will be used as a reference for the artificial neural network to be able to tell whether there is a distortion or not; if a distortion or a change in the signal happens, that will be an indicator of a possible blood clot. Fast Fourier Transform was taken from the reference signal and from the six other captured signals. The artificial neural network was trained with the available data to detect any potential blood clots and predict their locations. As shown in table 4.4. The used weights values for the input neurons.

Table 4.4. Weight values of the multi-layer perceptron's input neurons.

0.6923	0.0554	0.3542	0.0706	0.5708	1.0798	0.3713	0.6441	0.7786	0.7054	1.1713
0.4817	0.5146	0.5001	0.0826	0.5052	1.3740	0.3433	0.1443	0.5520	0.3392	0.2764
0.2195	1.3790	2.5664	1.2365	0.7858	1.2772	4.4535	0.7832	2.0944	1.4725	1.5165
0.6079	0.0962	0.5704	0.5667	0.8026	0.3197	0.2990	0.5904	0.6192	0.3381	0.2009
0.6374	0.7073	0.6419	0.2456	0.3125	0.5680	0.0719	0.2879	0.7787	0.3128	0.1652

Using eleven neurons in the input layer means that eleven sample would be taken for each measurement. To be able to make a comparison between the signals, the amplitude of each signal

was calculated and plotted separately. Later on, the six different signals were plotted on the same graph as shown in Figure 4.20.

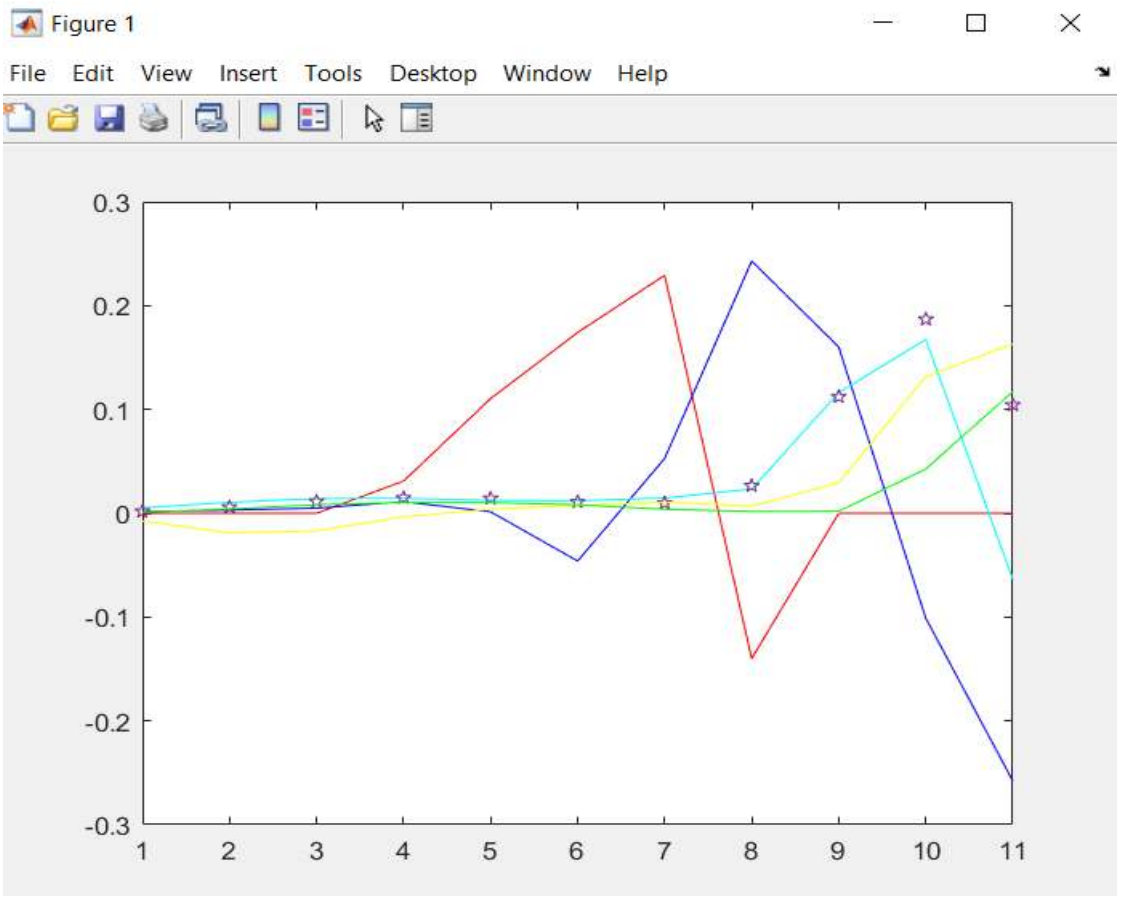

Figure 4.20. Six signals were plotted on the same graph.

As shown in Figure 4.21. both fitted curve and mean squared error were calculated and plotted, the fitting curve shows a linear graphic while the mean squared error shows that it took 7 epochs to get to the target value.

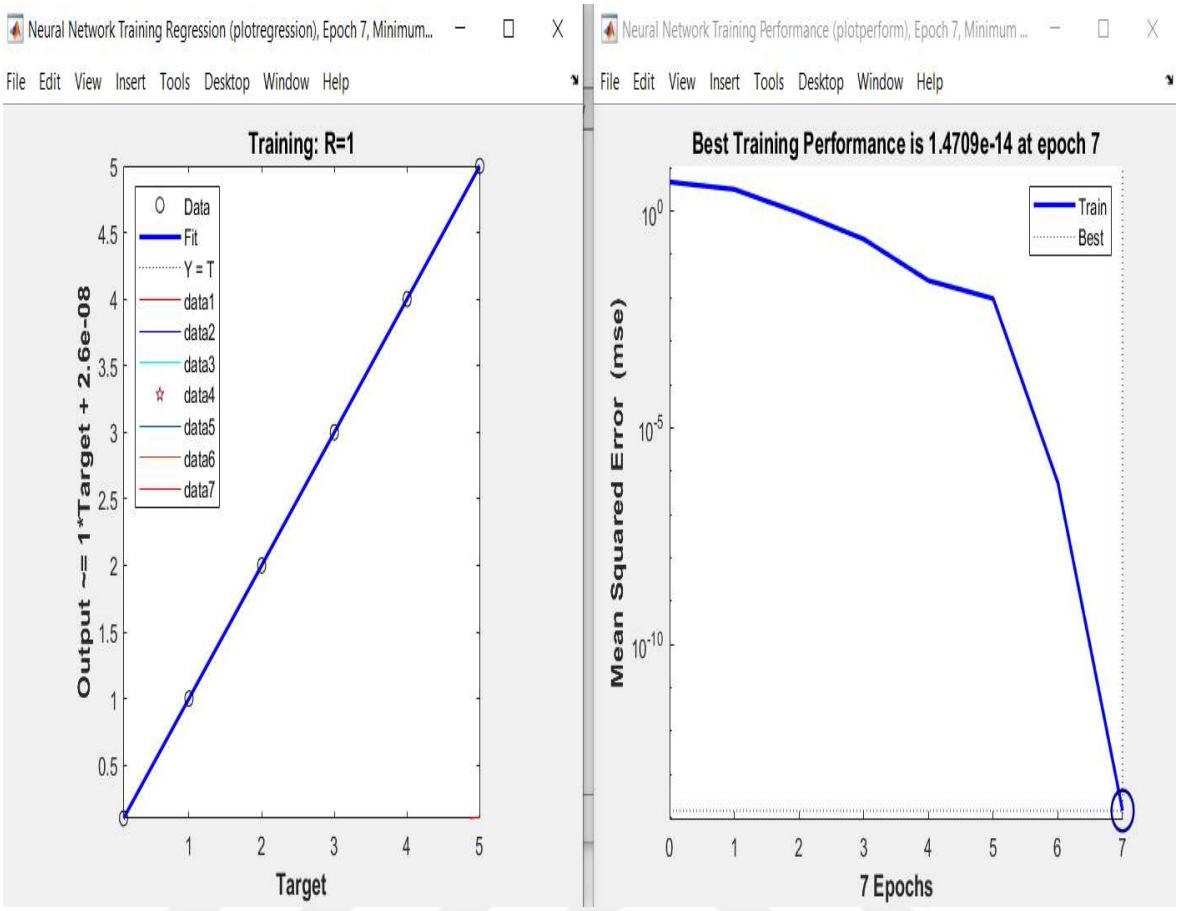

Figure 4.21. The fitting curve and the mean squared error curves.

Even though the results of the multi-layer perceptron were satisfying, however, as mentioned before the obtained data was captured as CSV files which make it difficult to understand the timeline of the clots when they pass through the transducer in respect to the timeline of the BCG signals and the potential distortion of the signals.

4.4. Embolus and fixed blood clots experiments

4.4.1. Embolus Experiment

In order to understand how blood clots affect blood flow in the blood vessels, an embolus experiment was conducted. In this experiment, a T connector tube was used to allow the liquid to flow between the two elastic tubes while simultaneously allowing the solder particles in the plastic cylinder, which represents the artificial embolus, to go into the main elastic tubes. At first, a transparent cylinder was used to contain the solder particles, as shown in Figure 4.22. However, due to the leaking in the cylinder, the experiment failed, and no results were obtained. Later, the transparent cylinder was replaced with another cylinder with less leaking, as shown in figure 4.23.

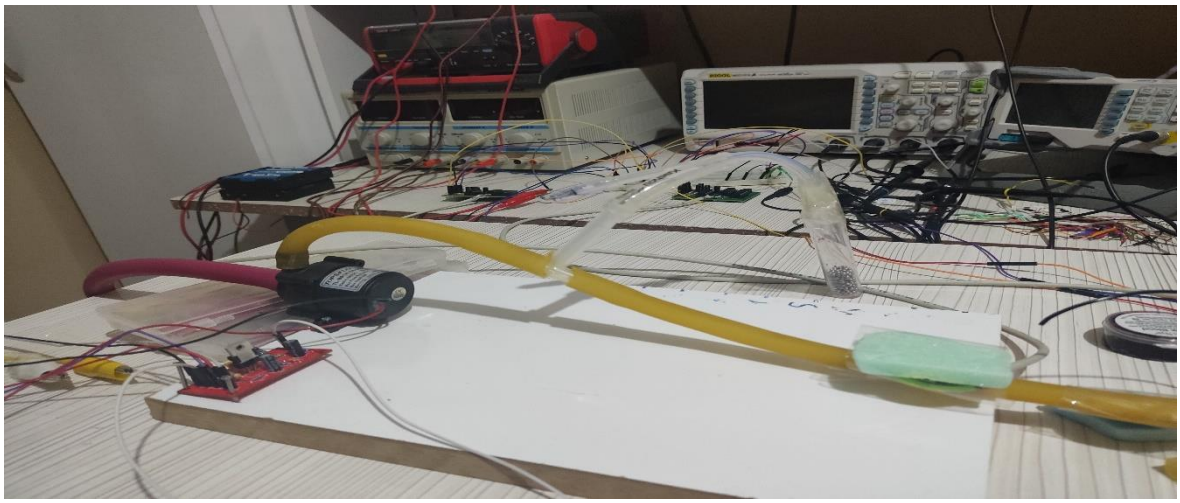

Figure 4.22. A transparent cylinder connected to the system through a T connector

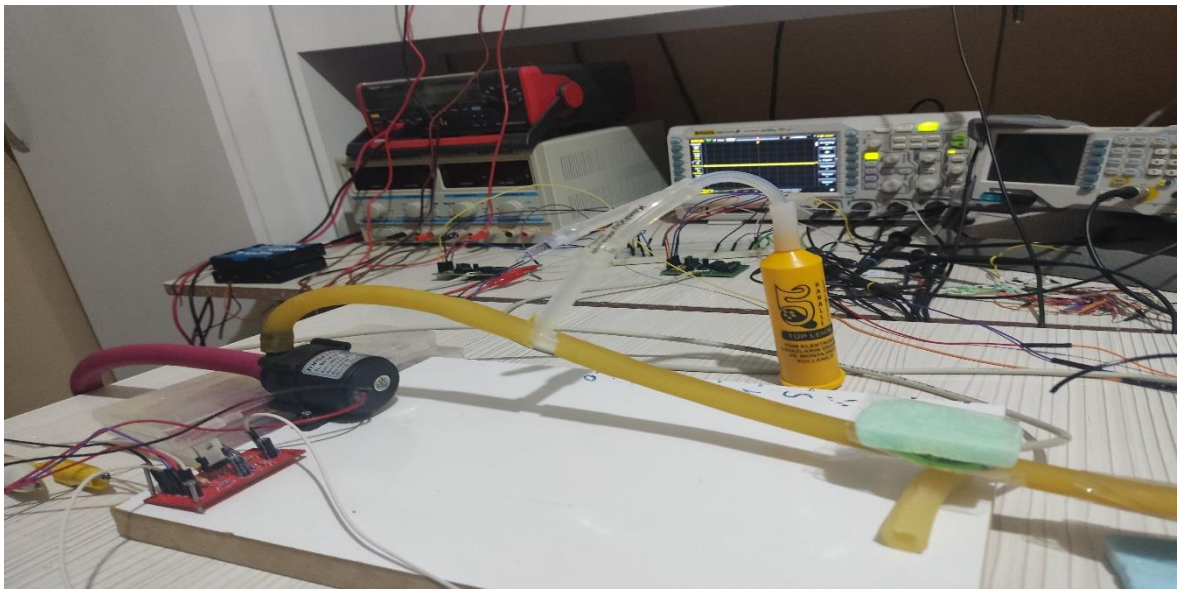

Figure 4.23. A new cylinder connected to the system through a T connector

The results from the embolus experiment showed that when an object such as an embolus flows through the blood and passes through the placement of the sensor generates a minor distortion in the signals. The distortion occurred as alternating high-frequency signals, as shown in Figure 4.24. and figure 4.25. Due to the complexity of the graphic and the fact that emboli have various shapes and sizes, the results of this experiment cannot be considered a clear-cut successful experiment; rather, it can be considered evidence of success regarding the current situation.

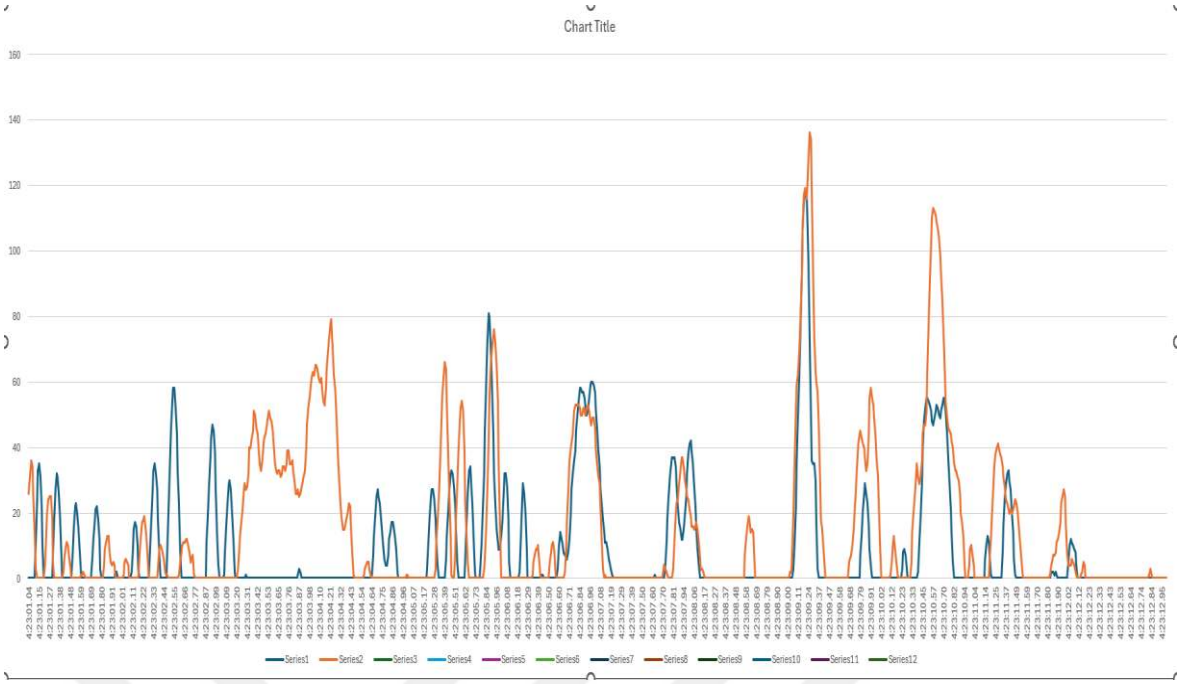

Figure 4.24. Emboli experiment graphic results zoomed out

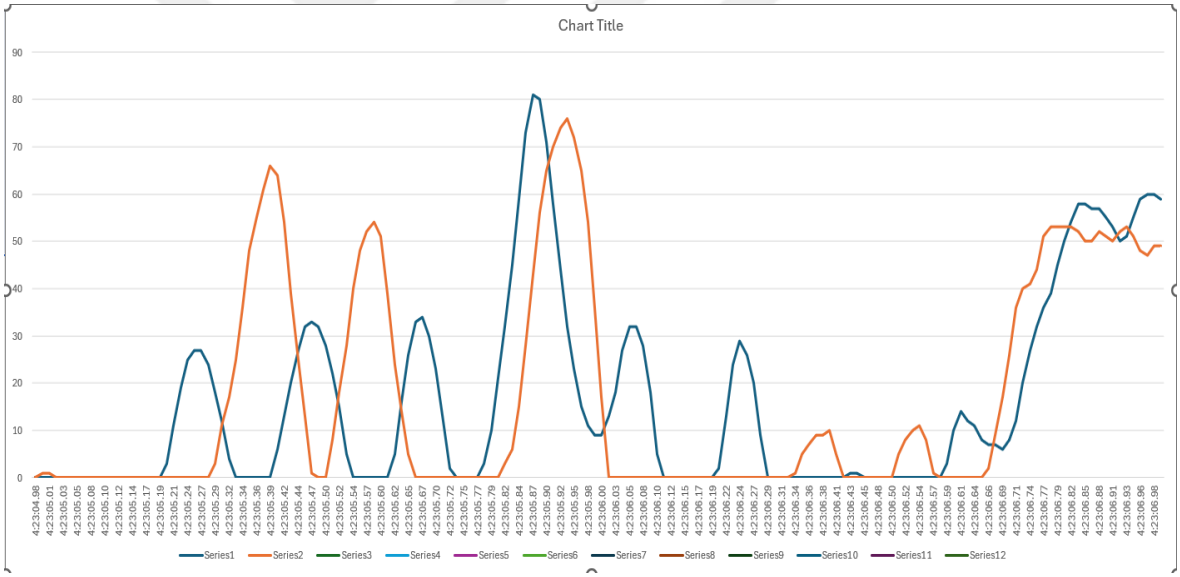

Figure 4.25. Emboli experiment graphic results zoomed in

4.4.2. Fixed blood clots experiments

Three different experiments were conducted to understand how fixed blood clots that adhere to the walls of the various types of blood vessels affect both blood flow and blood pressure; these experiments will also be useful to indicate whether the blood clots can interrupt the BCG signals or not. Each of these experiments was done multiple times to check whether the experiments would give the same results or not. Each of these experiments starts with opening the fossil, which allows the water to flow from the first bottle to the second bottle through an elastic tube. Two piezoelectric sensors are placed under the elastic tube in different locations. The distance between the two sensors is 6 cm, and each sensor is connected to a BCG circuit. After the faucet is opened, the water will start

to flow at a slow speed with a low pressure. Then, the TOPSFLOW pump will be turned on to pump the water with higher pressure and speed; when the water flows through the elastic tube and passes the locations of the placed sensors, each sensor will measure a signal. Figure 4.26. shows the obtained signals from the sensors when there is no blood clots in the system.

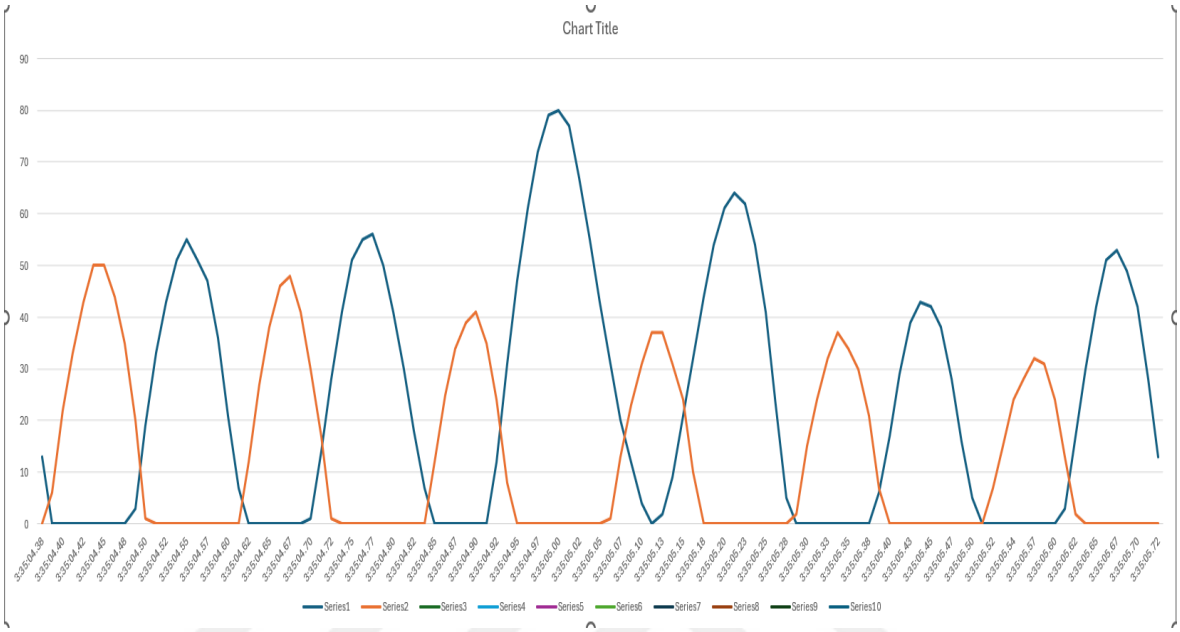

Figure 4.26. The two obtained signals from the piezoelectric sensors.

The signals are alternating due to the placements of the sensors, since the sensors are placed in different locations then one of the sensors will generate a signal before the other sensor do, the peak values of the first and the second signals are almost the same. While the obtained graphics provide data on the peak values and the timeline the difference in length between the two sensors is already known. The next three experiments will show the placement of the artificial blood clot and the resulting graphics.

In the first experiment the artificial blood clot was inserted and placed inside the elastic tube in the same location as the first peizoelectric sensor as shown in figure 4.27.

As shown in Figure 4.28. the pressure in the first location is higher compared to the second location; in other words, the first sensor is measuring a signal, and the second sensor is not measuring a lot of signals. The explanation for this is that when a blood clot is placed in the same location as the first sensor, the blood clot blocks the way fully or partially, which results in the accumulation of blood right before the first location. This accumulation leads to an increase in the peak value of the pressure signal, which is, in this case, the BCG signal.

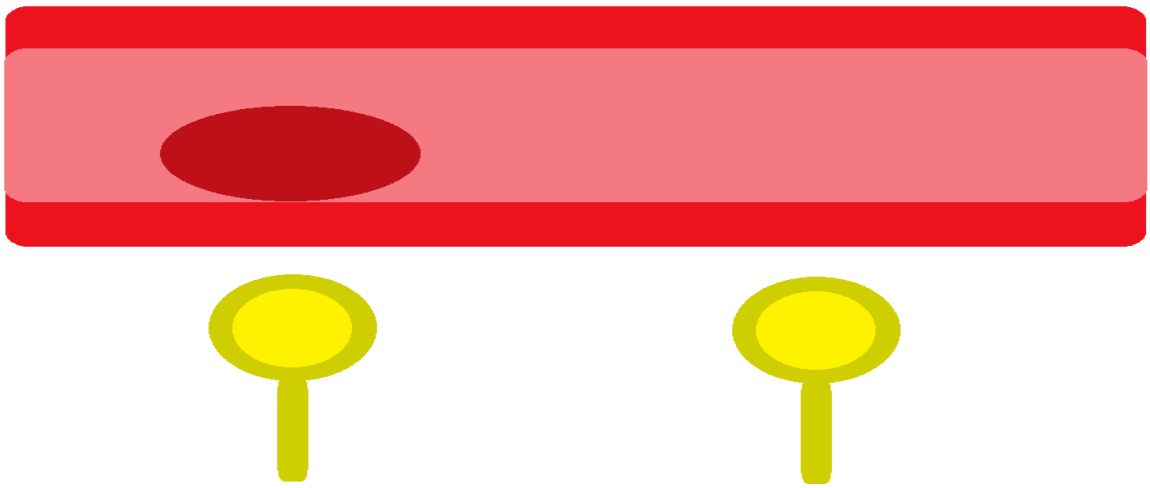

Figure 4.27. Artificial blood clot first location.

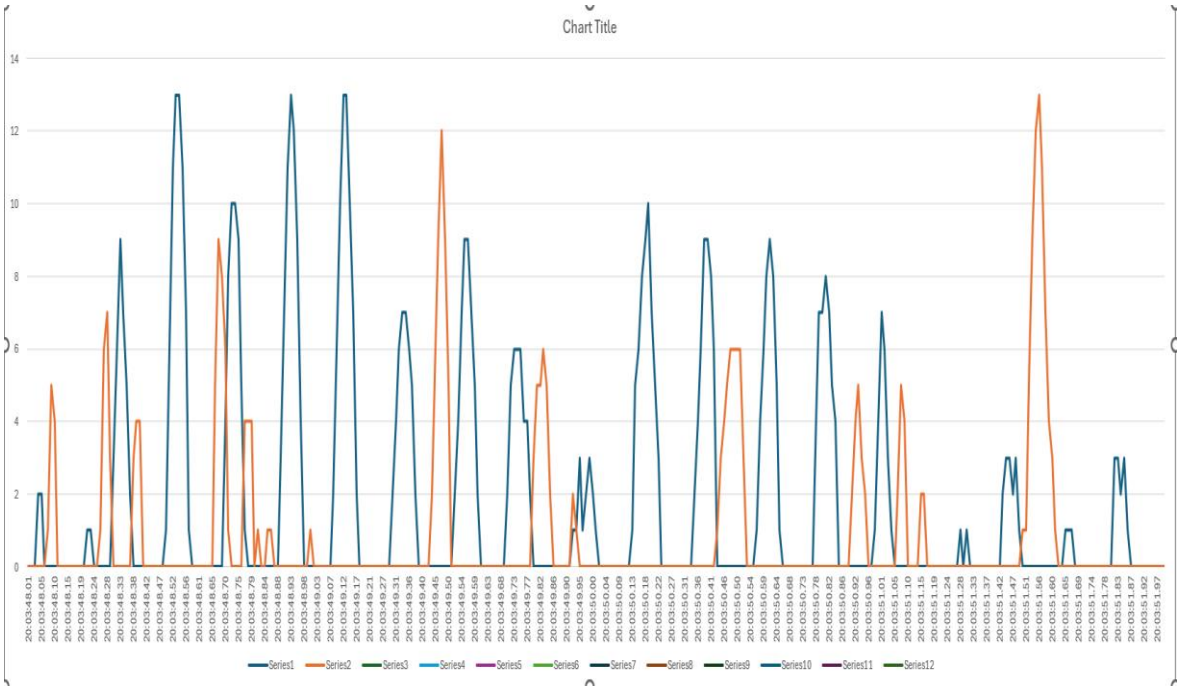

Figure 4.28. The obtained results from the first fixed blood clots experiment

In the second experiment, the artificial blood clot was inserted and placed in the same location as the second sensor, as shown in Figure 4.29. and the experiment was repeated to get the new results shown in figure 4.30.

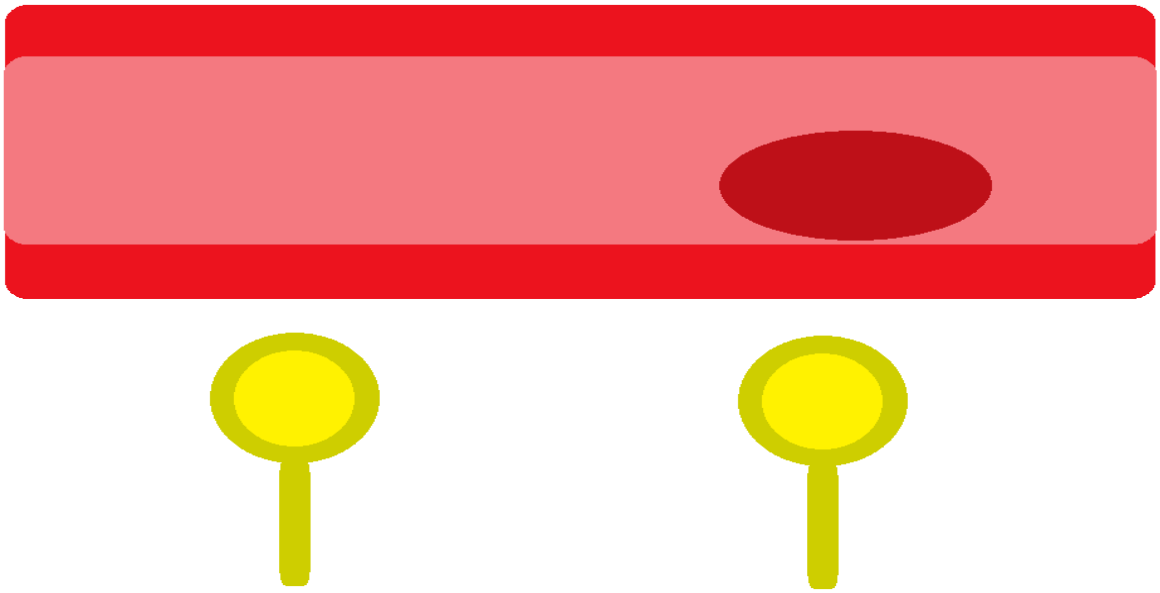

Figure 4.29. Artificial blood clot second location.

In the second experiment the amplitude and peak values of the first signal are higher than those of the second signal. That is due to the blocking of the tube and letting the liquid accumulate before reaching that point, which puts more pressure on the first sensor.

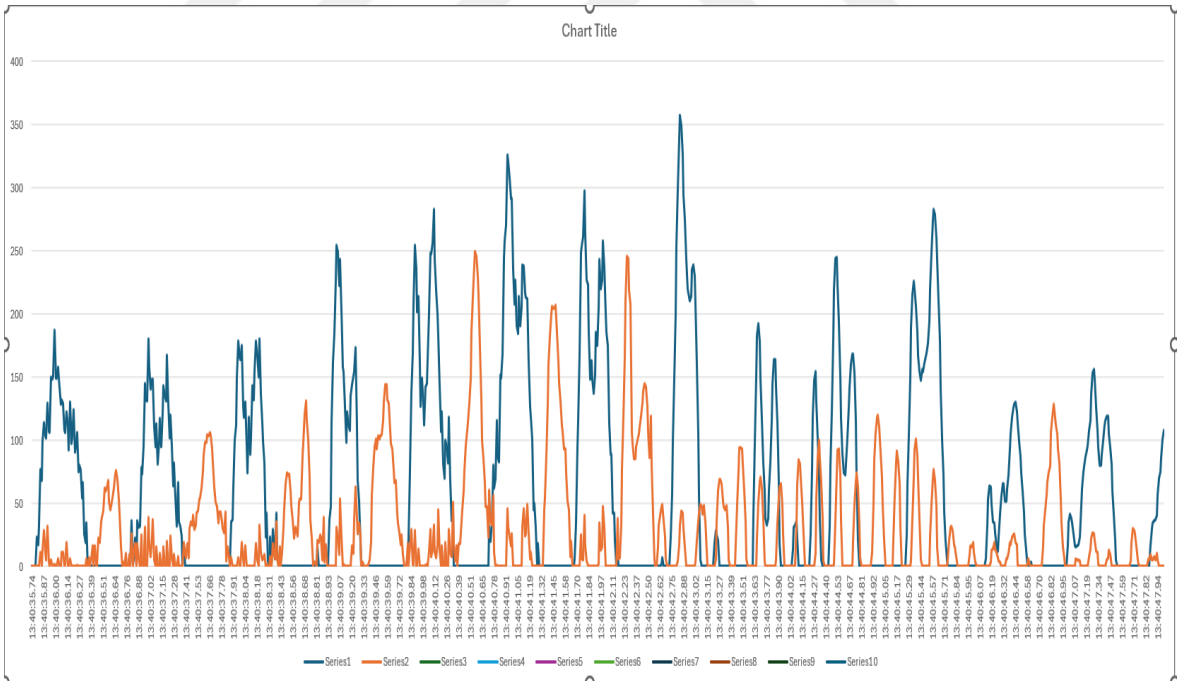

Figure 4.30. The obtained results from the second fixed blood clots experiment

In the last experiment, two blood clots were inserted and placed in the same locations as the first and second sensors, as shown in Figure 4.31. The obtained results from this experiment show that both sensors are barely measuring any signals, as in Figure 4.32. The reason for that is that those two artificial blood clots are almost fully blocking the elastic tube which focuses all the pressure

before the location of the first sensor. From time to time some liquid would flow through the blockage generating some low amplitude signals.

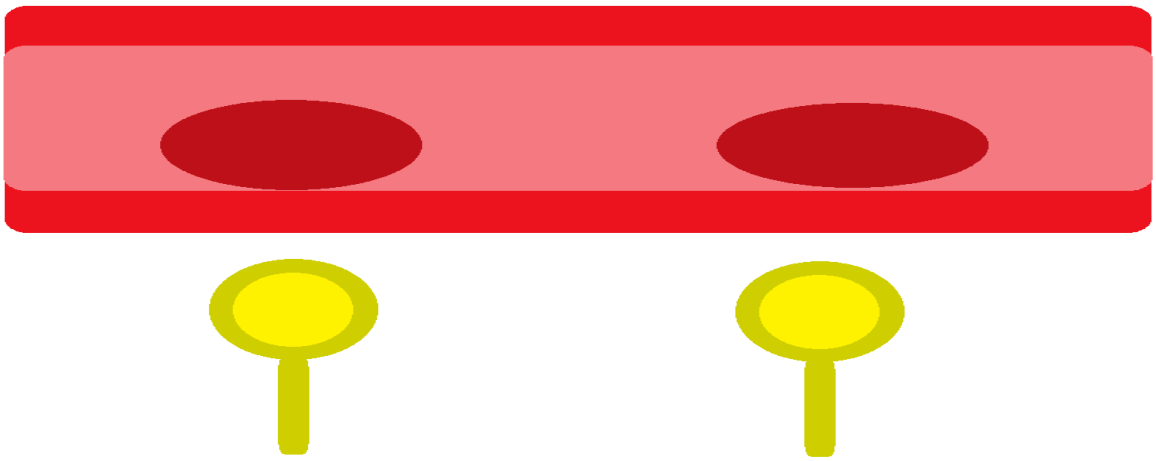

Figure 4.31. Artificial blood clots first and second locations.

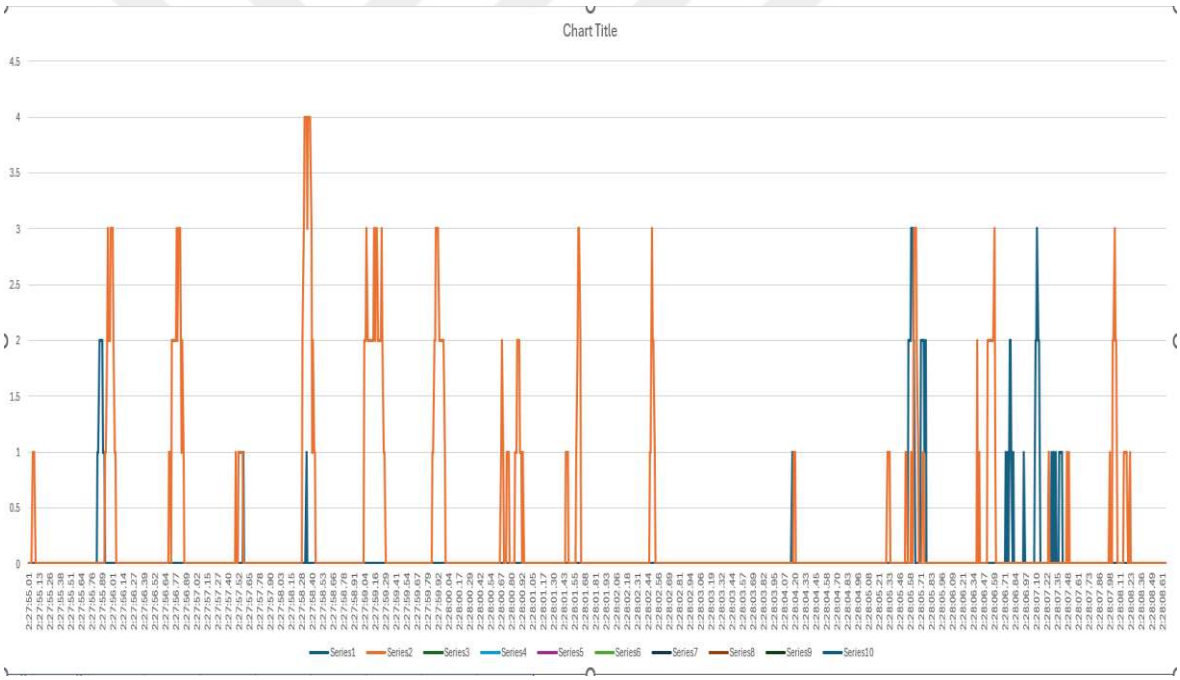

Figure 4.32. The obtained results from the third fixed blood clots experiment

5. CONCLUSIONS

This experiment shows that when a clot passes through an artery where there is a located transducer or from a near point, it is possible to detect the clot. In a completed system where an array of transducers will be used, the detection of blood clots will be more efficient, and it will help clinicians in the early detection of blood clots. There is no way to use the PCG signals as input data for the ANN to detect the potential blood clots because the PCG signal is a complex signal with a lot of changing parameters. However, the PCG signals can be forwarded to a power amplifier circuit connected to a speaker so they can be converted from electrical signals to sound signals. At that point a clinician would be able to tell whether there is a blood clot or not depending on the generated sound. A distortion in the PCG signal would be very difficult to detect from the graphics, so if there is any distortion, it would be much easier to tell since any distortion in the signal would be reflected as a distorted sound.

As for the experiment itself there are some steps that can be done to achieve better results. For example, the material of the tubes of the peristaltic pump can be selected from materials that have similar properties just like real blood vessels such as elasticity. In the same way instead of using water as a fluid to demonstrate the blood flow, another fluid can be selected that has similar properties.

In the proposed system, most of the processing methods were analog. Using digital filters and a microcontroller in addition to the array of transducers would give much more satisfying results with higher accuracy and less error, especially since multiple factors, such as the respiratory signal, would play a big role in distorting the measurements.

In future studies it would make sense to synchronise both BCG and PCG signals to understand the biological events more and extract what can be extracted as useful data for research. In the same way synchronizing the BCG with the ECG would give us more understanding of the cardiac cycle such as the R-J interval and more.

When it comes to the electronic circuit, there are some adjustments to make in order to make the system more efficient, such as adding elements that can protect the circuit from high voltages. Power analysis should also be done to understand how much current each element is drawing and how much power is dissipated. Electromagnetic compatibility is another form of protection for the circuit. If the device is going to work with batteries, then batteries with a high discharge current should be chosen. Otherwise, if the device is going to be connected to an electrical outlet, then a transformer with a full wave rectifier should be added to the circuit. The measured signals can vary regarding the place of measurement or from one person to another; that’s why an automatic gain control feature can be added for further improvement.

REFERENCES

Acharya, U. R., Fujita, H., Lih, O. S., Adam, M., Tan, J. H., & Chua, C. K. (2017). Automated detection of coronary artery disease using different durations of ECG segments with convolutional neural network. *Knowledge-Based Systems*, *132*, 62–71. https://doi.org/https://doi.org/10.1016/j.knosys.2017.06.003

Acharya, U. R., Fujita, H., Lih, O. S., Hagiwara, Y., Tan, J. H., & Adam, M. (2017). Automated detection of arrhythmias using different intervals of tachycardia ECG segments with convolutional neural network. *Information Sciences*, *405*, 81–90. https://doi.org/https://doi.org/10.1016/j.ins.2017.04.012

Acharya, U. R., Fujita, H., Oh, S. L., Hagiwara, Y., Tan, J. H., & Adam, M. (2017). Application of deep convolutional neural network for automated detection of myocardial infarction using ECG signals. *Information Sciences*, *415–416*, 190–198. https://doi.org/https://doi.org/10.1016/j.ins.2017.06.027

Acharya, U. R., Fujita, H., Oh, S. L., Raghavendra, U., Tan, J. H., Adam, M., Gertych, A., & Hagiwara, Y. (2018). Automated identification of shockable and non-shockable life-threatening ventricular arrhythmias using convolutional neural network. *Future Generation Computer Systems*, *79*, 952–959. https://doi.org/https://doi.org/10.1016/j.future.2017.08.039

Acharya, U. R., Oh, S. L., Hagiwara, Y., Tan, J. H., Adam, M., Gertych, A., & Tan, R. S. (2017). A deep convolutional neural network model to classify heartbeats. *Computers in Biology and Medicine*, *89*, 389–396. https://doi.org/https://doi.org/10.1016/j.compbiomed.2017.08.022

Alkhodari, M., & Fraiwan, L. (2021). Convolutional and recurrent neural networks for the detection of valvular heart diseases in phonocardiogram recordings. *Computer Methods and Programs in Biomedicine*, *200*, 105940. https://doi.org/https://doi.org/10.1016/j.cmpb.2021.105940

Alonso, E., Irusta, U., Aramendi, E., & Daya, M. R. (2020). A Machine Learning Framework for Pulse Detection During Out-of-Hospital Cardiac Arrest. *IEEE Access*, *8*, 161031–161041. https://doi.org/10.1109/ACCESS.2020.3021310

Balali, P., Rabineau, J., Hossein, A., Tordeur, C., Debeir, O., & Borne, P. (2022). Investigating Cardiorespiratory Interaction Using Ballistocardiography and Seismocardiography—A Narrative Review. *Sensors*, *22*, 9565. https://doi.org/10.3390/s22239565

Chen, G., & Yang, R. (2018). *Electronic Acoustic Stethoscope with ECG*.

Evans, P. A., Hawkins, K., Williams, P. R., & Williams, R. L. (2008). Rheometrical detection of incipient blood clot formation by Fourier transform mechanical spectroscopy. *Journal of Non-Newtonian Fluid Mechanics*, *148*(1), 122–126. https://doi.org/https://doi.org/10.1016/j.jnnfm.2007.04.020

Fuchs, G., Berg, N., Eriksson, A., & Prahl Wittberg, L. (2016). Detection of Thrombosis in the Extracorporeal Membrane Oxygenation Circuit by Infrasound: Proof of Concept. *Artificial Organs*, *41*. https://doi.org/10.1111/aor.12782

Gherson, P., Eherts, R. W., & Pernicano, T. (2000). *Blood clot detector*. https://patents.google.com/patent/US6022747A/en

Hameed, S., Hasan, J., & Khalil, E. (2022). Photoacoustic technique for diagnosis of blood clotting. *International Journal of Health Sciences*. https://doi.org/10.53730/ijhs.v6nS4.11834

He, D., Winokur, E., & Sodini, C. (2012). An Ear-worn Continuous Ballistocardiogram (BCG) Sensor for Cardiovascular Monitoring. *Conference Proceedings : ... Annual International Conference of the IEEE Engineering in Medicine and Biology Society. IEEE Engineering in Medicine and Biology Society. Conference*, *2012*, 5030–5033. https://doi.org/10.1109/EMBC.2012.6347123

Inan, O., Migeotte, P.-F., Park, K., Etemadi, M., Tavakolian, K., Casanella, R., Zanetti, J., Tank, J., Funtova, I., Prisk, K., & Di Rienzo, M. (2014). Ballistocardiography and Seismocardiography: A Review of Recent Advances. *IEEE Journal of Biomedical and Health Informatics*, *19*. https://doi.org/10.1109/JBHI.2014.2361732

Juratli, M., Menyaev, Y., Sarimollaoglu, M., Melerzanov, A., Nedosekin, D., Culp, W., Suen, J., Galanzha, E., & Zharov, V. (2018). Noninvasive label-free detection of circulating white and red blood clots in deep vessels with a focused photoacoustic probe. *Biomedical Optics Express*, *9*, 5667. https://doi.org/10.1364/BOE.9.005667

Kacmaz, S., Ercelebi, E., Zengin, S., & Cindoruk, S. (2017). The use of infrared thermal imaging in the diagnosis of deep vein thrombosis. *Infrared Physics & Technology*, *86*, 120–129. https://doi.org/https://doi.org/10.1016/j.infrared.2017.09.005

Khurshid, H., Friedman, B., Berwin, B., Shi, Y., Ness, D., & Weaver, J. (2017). Blood clot detection using magnetic nanoparticles. *AIP Advances*, *7*, 056723. https://doi.org/10.1063/1.4977073

Krishnan, H., Md A, M. K., Zulhaimi, H., Anbu, P., & Subramaniam, S. (2022). Molecularly Imprinted Polymer Enhances Affinity and Stability Over Conventional Aptasensor for Blood Clotting Biomarker Detection on Regimented Carbon Nanohorn and Gold Nanourchin Hybrid Layers. *Sensors and Actuators B: Chemical*, *363*, 131842. https://doi.org/10.1016/j.snb.2022.131842

Li, Z., Zhou, D., Wan, L., Li, J., & Mou, W. (2020). Heartbeat classification using deep residual convolutional neural network from 2-lead electrocardiogram. *Journal of Electrocardiology*, *58*, 105–112. https://doi.org/https://doi.org/10.1016/j.jelectrocard.2019.11.046

Liu, S.-H., Chen, W., Su, C.-H., & Pan, K.-L. (2022). Convolutional neural Network-based detection of deep vein thrombosis in a low limb with light reflection rheography. *Measurement*, *189*, 110457. https://doi.org/https://doi.org/10.1016/j.measurement.2021.110457

Liu, S.-H., Wang, J.-J., Chen, W., Pan, K., & Su, C.-H. (2021). An Examination System to Detect Deep Vein Thrombosis of a Lower Limb Using Light Reflection Rheography. *Sensors*, *21*, 2446. https://doi.org/10.3390/s21072446

Mary, S., Kambhamettu, C., & Barner, K. (2018). A novel application of deep learning for single-lead ECG classification. *Computers in Biology and Medicine*, *99*. https://doi.org/10.1016/j.compbiomed.2018.05.013

Mohktar, M., Ibrahim, F., & Ismail, N. (2013). Non-invasive approach to predict the cholesterol level in blood using bioimpedance and neural network techniques. *Biomedical Engineering: Applications, Basis and Communications*, *25*, 1350046. https://doi.org/10.4015/S1016237213500464

Oldenburg, A., Wu, G., Spivak, D., Tsui, F., Wolberg, A., & Fischer, T. (2011). Imaging and Elastometry of Blood Clots Using Magnetomotive Optical Coherence Tomography and Labeled Platelets. *IEEE Journal of Selected Topics in Quantum Electronics : A Publication of the IEEE Lasers and Electro-Optics Society*, *18*, 1100–1109. https://doi.org/10.1109/JSTQE.2011.2162580

Park, S.-H., & Lee, S.-P. (1998). EMG pattern recognition based on artificial intelligence techniques. *IEEE Transactions on Rehabilitation Engineering*, *6*(4), 400–405. https://doi.org/10.1109/86.736154

Parveen, F., & Wahid, P. (2022). Detection of Blood Clots inside the Brain using Microwave Imaging. *2022 3rd URSI Atlantic and Asia Pacific Radio Science Meeting (AT-AP-RASC)*, 1–4. https://doi.org/10.23919/AT-AP-RASC54737.2022.9814275

Rajput, J., Sharma, M., Kumbhani, D., & Acharya, U. R. (2021). Automated detection of hypertension using wavelet transform and nonlinear techniques with ballistocardiogram signals. *Informatics in Medicine Unlocked*, *26*, 100736. https://doi.org/10.1016/j.imu.2021.100736

Sanders, L., & Reddy, Y. (2007). Detecting Blood Clots using Neural Networks. In *Proceedings - International Conference on Information Technology-New Generations, ITNG 2007*. https://doi.org/10.1109/ITNG.2007.73

Singh, M., & Cheema, A. (2013). Heart Sounds Classification using Feature Extraction of Phonocardiography Signal. *International Journal of Computer Applications*, *77*, 13–17. https://doi.org/10.5120/13381-1001

Śmigiel, S., Pałczyński, K., & Ledzinski, D. (2021). Deep Learning Techniques in the Classification of ECG Signals Using R-Peak Detection Based on the PTB-XL Dataset. *Sensors*, *21*, 8174. https://doi.org/10.3390/s21248174

Song, J., Kang, X., Wang, L., Ding, D., Kong, D., Li, W., & Qi, J. (2023). Near-infrared-II photoacoustic imaging and photo-triggered synergistic treatment of thrombosis via fibrin-

specific homopolymer nanoparticles. *Nature Communications*, *14*(1), 6881. https://doi.org/10.1038/s41467-023-42691-8

Topcuoglu, M., & Arsava, E. M. (2012). Neurosonology of emboli detection and monitoring. *Turk Serebrovaskuler Hastaliklar Dergisi*, *18*, 59–71.

Varghees, N., & K I, R. (2014). A novel heart sound activity detection framework for automated heart sound analysis. *Biomedical Signal Processing and Control*, *13*, 174–188. https://doi.org/10.1016/j.bspc.2014.05.002

Yang, X., Zhang, X., Yang, M., & Zhang, L. (2021). 12-Lead ECG arrhythmia classification using cascaded convolutional neural network and expert feature. *Journal of Electrocardiology*, *67*, 56–62. https://doi.org/https://doi.org/10.1016/j.jelectrocard.2021.04.016

CURRICULUM VITAE

Name Surname:	NADIM ALDARVISH
Languages:	TURKISH, ARABIC, ENGLISH, FRENCH
Education	
High School:	Al Amal Private School, Syria / Aleppo, 2010-2013
	Amman National School, Jordan / Amman, 2013-2014
College:	University of Cukurova
	Faculty of Engineering
	Biomedical Engineering
	2015-2021
Previous Jobs:	Electronic Laboratory Private Lessons 2019-2023